LLNL-JRNL-2015082

Lawrence Livermore National Laboratory

Remote Influence of Andean Convection on Amazonian Rainfall and Its Mechanisms

J Bacmeister, R Terai, H Qin, G Kiladis, P Bogenschutz, M Pritchard

January 2026

Journal of Geophysical Research: Atmospheres

Disclaimer

This work performed under the auspices of the U.S. Department of Energy by Lawrence Livermore National Laboratory under Contract DE-AC52-07NA27344.

An edited version of this paper was published by AGU. Published (2025) American Geophysical Union.
Qin, H., Pritchard, M., Terai, C. R., Bacmeister, J., Bogenschutz, P., & Kiladis, G. N. (2025). Remote influence of Andean convection on Amazonian rainfall and its mechanisms. Journal of Geophysical Research: Atmospheres, 130, e2025JD043465. https://doi.org/10.1029/2025JD043465

Remote Influence of Andean Convection on Amazonian Rainfall and Its Mechanisms

Hongchen Qin[1]*, Michael Pritchard[1], Christopher R. Terai[2], Julio Bacmeister[3], Peter Bogenschutz[2], George N. Kiladis[4]

[1]University of California Irvine, Irvine, California.

[2]Lawrence Livermore National Laboratory, Livermore, California.

[3]National Center for Atmospheric Research, Boulder, Colorado.

[4]Earth System Research Laboratory, Physical Sciences Division, National Oceanic and Atmospheric Administration, Boulder, Colorado.

*Current: University of Connecticut

Corresponding author: Hongchen Qin (hongcheq@uci.edu)

Key Points:

- Andean convective forcing notably reduces Amazonian rainfall at the weather timescale.
- Changes in the moisture budget and thermodynamics drive precipitation responses over the Amazon.
- Andean east flank descending anomalies propagate eastward and cause vertical advective drying over the Amazon.

Abstract

Models from Coupled Model Intercomparison Project Phase 6 produce too much precipitation over the Andes but too little over the Amazon, or the Wet Andes–Dry Amazon (WADA) bias pattern. Unlike the conventional view that convection parameterization and land model deficiencies can contribute to Amazonian rainfall biases, we approach this long-standing biased model behavior through the lens of Andean convection. Using Community Earth System Model v1.1 and focusing on the wet season, our mechanism-denial experiments demonstrate that Andean convection notably reduces precipitation over the Amazon during austral summer. The Andean forced Amazonian response operates on weather timescale. The reduction of Amazonian rainfall is detectable within a few hours after initial Andean forcing. The precipitation response is primarily driven by variations in the moisture budget and is moderated by changes in convective available potential energy over the Amazon. Changes in the total advection of moisture over the Amazon are dominated by the vertical advection term and can be attributed to discrepancies in the dynamic omega field. In the experiments, the Andean east flank region is scrutinized where the vertical velocity and moisture fields play an intermediary role for the Andean driven WADA connection. The Andean forcing induces descending

An edited version of this paper was published by AGU. Published (2025) American Geophysical Union.
Qin, H., Pritchard, M., Terai, C. R., Bacmeister, J., Bogenschutz, P., & Kiladis, G. N. (2025). Remote influence of Andean convection on Amazonian rainfall and its mechanisms. Journal of Geophysical Research: Atmospheres, 130, e2025JD043465. https://doi.org/10.1029/2025JD043465

anomalies on the Andean east flank. The disturbances of wind and geopotential fields over the Andean east flank propagate eastward via Kelvin waves. Over the Amazon, descending anomalies and advective drying lead to reduction of mid-to-high level cloud, increase of shortwave cloud forcing and surface net radiation, enhancement of themodynamic stability and rainfall reduction.

Plain Language Summary

Contemporary climate models have biases in simulating precipitation over the South American region, they produce too much rain over the Andes but not enough over the Amazon. Unlike previous studies, we investigate this issue from the lens of Andean-driven mechanism by designing numerical simulations where the impacts of Andean convection can be carefully studied. The results indicate that Andean convection could suppress precipitation over the Amazon in the climate model via its effects on moisture advection and atmospheric instabilities. The Andean-driven mechanism can propagate eastward towards the Amazon via equatorial wave activities.

1 Introduction

As the largest terrestrial carbon reservoir, the Amazon rainforest is critical to the climate and the Earth system. To understand its future, especially as the community approaches an era of explicitly simulated vegetation, it is crucial for Earth System Models (ESMs) to accurately capture the physical processes that sculpt the hydrological cycle in Amazonia. A realistic representation of Amazonian hydroclimate is also instrumental to climate non-locally, as Amazonian rainfall significantly modulates the hydrological cycle and energy balance globally (Avissar & Werth, 2005; Lawrence & Vandecar, 2015; Medvigy et al., 2013; Snyder, 2010; Werth & Avissar, 2002). However, the current understanding of the processes that control Amazonian rainfall in present and future climate remains incomplete.

Symptoms of such incomplete understanding are partly reflected in chronic ESM biases; modern climate models do not simulate rainfall realistically over tropical South America. Specifically, the multi-model annual mean rainfall from the Coupled Model Intercomparison Project Phase 5 (CMIP5) suffers from a “Wet Andes–Dry Amazon (WADA)” bias (IPCC, 2014; Mehran et al., 2014), which is associated with too much surface net radiation, overly high Bowen ratio over the Amazon, and excessive rainfall along the Intertropical Convergence Zone (ITCZ) in adjacent oceans, and erroneous interactions among different drivers (Yin et al., 2012). This WADA bias pattern also stubbornly exists in CMIP6 simulations (IPCC AR6 WGI, Figure 3.13 therein, Eyring et al.). Although Sea Surface Temperature (SST) and its distributions are known to influence Amazonian hydroclimate (Chen et al., 2018; Fernandes et al., 2015; Yin et al., 2012), the existence of this WADA symptom in CMIP6 simulations following the Atmospheric Model Intercomparison Project (AMIP) protocol (Figure 1a,b) suggests its non-oceanic sources of bias and the dryness is accompanied by severe underestimates of lower tropospheric humidity over the Amazon (Lintner et al., 2017).

An edited version of this paper was published by AGU. Published (2025) American Geophysical Union.
Qin, H., Pritchard, M., Terai, C. R., Bacmeister, J., Bogenschutz, P., & Kiladis, G. N. (2025). Remote influence of Andean convection on Amazonian rainfall and its mechanisms. Journal of Geophysical Research: Atmospheres, 130, e2025JD043465. https://doi.org/10.1029/2025JD043465

From the atmospheric perspective, the rainfall dry biases over the Amazon may be partially caused by model convection treatments. Sakaguchi et al. (2018) showed that wet season rainfall dry biases over southwestern Amazon are very sensitive to the convective available potential energy calculation in the deep convection scheme. Based on a short hindcast approach, Ma et al. (2021) found the wet-season precipitation dry bias over the Amazon in Community Atmosphere Model v5 (CAM5) is due to severe underestimates of late afternoon rainfall and nighttime convective regimes in the model, which is mainly caused by convection parameterization. Unsurprisingly, in the fully coupled Community Earth System Model v1 (CESM v1) large ensemble simulations where CAM5 is the atmospheric component, the Amazon wet-season negative precipitation bias is also detected (Thome Sena & Magnusdottir, 2020). Indeed, the wet-season dry bias over the Amazon in CAM5 can be alleviated by optimized deep convection triggering via using dynamic convective available potential energy and the unrestricted launch level trigger (Cui et al., 2021; S. C. Xie et al., 2019). In the CESM v2, Meehl et al. (2020) found that Amazonian wet-season precipitation can be increased via modifications to increase the sensitivity of deep convection to lower tropospheric humidity in the ZM deep convection scheme (Zhang & Mcfarlane, 1995). Furthermore, a multitude of cloud-resolving model simulations with various purposes have demonstrated improvements in Amazonian hydroclimate. For instance, using the Weather Research and Forecasting (WRF) model with prescribed large-scale circulation based on weak temperature gradient, the morning fog layer in the wet-season and associated cloud albedo feedbacks are captured, which contributes to better representations of the diurnal and seasonal cycles of surface fluxes and precipitation over the Amazon (Anber et al., 2015); using 2D Cloud-Resolving Models embedded in traditional General Circulation Model (GCM), cloud super-parameterization is shown to generally improve the soil moisture – evapotranspiration (ET) relationship and surface turbulent fluxes (Qin et al., 2018; Sun & Pritchard, 2016) and to reduce the wet-season rainfall dry bias over southern Amazon with a higher-order turbulence closure scheme (K. Zhang et al., 2017).

From the terrestrial point of view, Yin et al. (2012) speculated that overly strong ET during the wet season due to excessive surface net radiation might cause excess soil moisture loss, which could subsequently cause a scarcity of ET and rainfall in the following dry season. Under the CESM lineage, K. Zhang et al. (2017) argued that unlike during the wet season, dry season rainfall dry biases over southern Amazon is largely driven from the land component. Regarding the wet season rainfall deficit over southwestern Amazon in CESM v1, Sakaguchi et al. (2018) shows that despite improvements in surface turbulent fluxes, the rainfall biases are not relieved by replacing Community Land Model version 4 (CLM4) with CLM4.5, suggesting that the biases might be common in both versions of the land model.

It is tempting to view the causality connecting Amazonian and Andean rainfall from east to west, i.e., with the mean flow and moisture transport. This is logical, as the South American Low-Level Jet (SALLJ) transports massive moisture from the Atlantic Ocean to Amazonia and then onto the Andes during austral summer. In other words, the SALLJ is a direct contributor to precipitation. In fact, the rainfall maximum at the Peruvian Andes–Amazon transition is found right at the height of around 1000m, at the level where the SALLJ peaks (Chavez & Takahashi,

An edited version of this paper was published by AGU. Published (2025) American Geophysical Union.
Qin, H., Pritchard, M., Terai, C. R., Bacmeister, J., Bogenschutz, P., & Kiladis, G. N. (2025). Remote influence of Andean convection on Amazonian rainfall and its mechanisms. Journal of Geophysical Research: Atmospheres, 130, e2025JD043465. https://doi.org/10.1029/2025JD043465

2017). Interesting positive feedbacks accompany this east-to-west moisture transport. For example, latent heat release from precipitation over the Amazon helps strengthen the atmospheric heating gradient between the Amazon and the tropical Atlantic Ocean, which can further enhance the moisture inflow (Boers et al., 2017; Kooperman et al., 2018). The argument of using SALLJ moisture transport to understand Andean and Amazonian rainfall is evident in studies focusing on climate of the past, present, and future. During the Last Glacial Maximum, the strengthening of the Amazon-to-Andes moisture transport was found responsible for rainfall enhancement over Peruvian and Bolivian Andes and large-scale drying over the Amazon (Vizy & Cook, 2007). In the more recent historical climate, overly weakened low-level flow into southern Amazonia is significantly correlated with the underestimation of rainfall during wet seasons among CMIP5 models (Barros & Doyle, 2018). With elevated CO_2 levels in future climate, the physiological response of Amazon rainforests drives a similar WADA response of rainfall (Kooperman et al., 2018) related to transport of moisture and Moist Static Energy (MSE) by the SALLJ (Langenbrunner et al., 2019).

Contrastingly, we focus on an alternate hypothesis – that some of the causality connecting the Andes and Amazon may flow in the *reverse* direction, i.e., from west-to-east against the mean flow. This hypothesis is intriguingly consistent with close links between Andean orography, SALLJ formation, and Amazon rainfall that are well established (Insel et al., 2010; Rasmussen & Houze, 2016) in regional modeling experiments. In CMIP6 models, the 500hPa Omega and humidity fields on the Andean east flank have significant correlation with Amazonian precipitation (Figure S1, Text S1). This implies a possible west-to-east control mechanism driven by Andean convection. The purpose of this article is to answer the question: can the WADA phenomenon be driven from the Andean side (rather than the Amazonian side)? In particular, whether or not Andean convection is capable of notably changing Amazonian rainfall, and if so, to understand the relevant mechanisms. By testing this hypothesis, we aim to better understand the role of orographic Andean convection on rainfall over tropical South America. Unlike regional modeling studies (Anber et al., 2015; Insel et al., 2010; Rasmussen & Houze, 2016), or CMIP5/CMIP6 studies (Baker & Spracklen, 2022; L. H. Li et al., 2018; Z. Li et al., 2022; Lintner et al., 2017; Mueller & Seneviratne, 2014; Yazdandoost et al., 2021; Yin et al., 2012), which heavily rely on diagnostic measures, we will use a global model to conduct causatively unambiguous sensitivity experiments. This will enable statistical detection and reliable investigation of the effects of Andean convection on Amazonian rainfall.

This article is structured as follows. Section 2 will briefly describe the methods and data to untangle and understand the effects of Andean convection on Amazonian precipitation, including experiment design, moisture budget analysis and decomposition of moisture advection. In Section 3, we examine diurnal features of precipition in the control simulation, Andean convective forcing characteristics, responses of Amazonian precipitation, and multiple perspectives to understand the underlying mechanisms. Section 4 depicts the Andean forced eastward field expansions towards the Amazon. Discussions are provided in Section 5. We summarize our results with conclusions in Section 6.

An edited version of this paper was published by AGU. Published (2025) American Geophysical Union.
Qin, H., Pritchard, M., Terai, C. R., Bacmeister, J., Bogenschutz, P., & Kiladis, G. N. (2025). Remote influence of Andean convection on Amazonian rainfall and its mechanisms. Journal of Geophysical Research: Atmospheres, 130, e2025JD043465. https://doi.org/10.1029/2025JD043465

2 Data and Methods

2.1 Experiment design

To investigate the role of Andean convection on Amazonian rainfall, we conduct two groups of simulations using CESM v1.1.1 with the F_AMIP_CAM5 compset. All simulations use the finite volume dynamical core at 1.9°x2.5° (f19_g16) horizontal resolution and 30 vertical levels with prescribed sea surface temperature and sea ice (i.e., AMIP-style). The simulations employ the standard "CAM5" physics parameterization suite. The deep convection parameterization follows Zhang and Mcfarlane (1995) with modifications from Richter and Rasch (2008) and Raymond and Blyth (1986, 1992); the shallow convection scheme uses the University of Washington shallow convection scheme following Park and Bretherton (2009); cloud microphysics based on Morrison and Gettelman (2008) with updates from Gettelman et al. (2010) and cloud macrophysics are from Park et al. (2014); radiative transfer calculations are given by the Rapid Radiative Transfer Method for GCMs, known as the RRTMG (Iacono et al., 2008; Mlawer et al., 1997). Aerosol concentration data is prescribed with cyclic values of the year 2000.

(1) CTR group: An AMIP-type simulation of Austral summer (Dec-Jan-Feb; DJF) of the year 1989-2008. The CTR group consists of 20 sets of simulations, each initialized on Nov 21st, with the first ten days discarded as spin-up.

(2) TOPO group: A sensitivity test ensemble, in which we artificially shut down the temperature tendency from parameterized deep, shallow convection, cloud microphysics, and cloud macrophysics over the Andean topography (methods described below). Each TOPO simulation lasts ten days with hourly output frequency and is branched off from the CTR simulation at 10-day increments starting from Dec 1st midnight UTC. For example, 1st TOPO simulation: 12/01/1989 – 12/10/1989, 2nd TOPO simulation: 12/11/1989 – 12/20/1989, 3rd TOPO simulation: 12/21/1989 – 12/30/1989, …, last TOPO simulation: 02/19/2009 – 02/28/2009. This strategy results in a 180-member (9-member per DJF) ensemble of paired 10-day hindcasts – differences between the ensemble mean of CTR and TOPO will isolate the effects of Andean convection with statistical clarity. The hindcasts are chosen to be 10 days because (a) earlier pilot test indicates that the Andean driven response over the Amazon has a timescale dependence, and (b) we want a larger number of CTR vs. TOPO comparisons within the limit of computational resources.

It is worth noting that our experiments design hinges on branching off with mechanism denial, we call each CTR and corresponding branched-off TOPO simulation as one ensemble-member-pair. In this context, the notion of ensemble differs from the typical forecasting ensemble whose purpose is to sample atmospheric chaos by perturbing initial conditions or changing model parameters/configurations.

The mechanism denial in the TOPO group is restricted geographically based on topographic height using a ramp function (Figure 2). We divide the surface geopotential height by the gravitational acceleration constant to compute surface topography height. At each model time step, we apply the ramp function to modulate the temperature tendency calculated by the deep, shallow convection schemes, cloud macrophysics, and microphysics packages. Full

An edited version of this paper was published by AGU. Published (2025) American Geophysical Union.
Qin, H., Pritchard, M., Terai, C. R., Bacmeister, J., Bogenschutz, P., & Kiladis, G. N. (2025). Remote influence of Andean convection on Amazonian rainfall and its mechanisms. Journal of Geophysical Research: Atmospheres, 130, e2025JD043465. https://doi.org/10.1029/2025JD043465

heating (no denial) is allowed at low elevations (h< 500). We linearly decrease the calculated temperature tendency in proportion to local topography when approaching higher elevations ($500m \leq h < 600m$), until reaching complete denial of parameterized temperature tendency where $h \geq 600m$. We use 500 and 600 meters to apply the ramp function because the corresponding applied area roughly covers the positive precipitation bias area over the Andes.

The reasons for conducting only wet-season (DJF) simulations are trifold. First, Andean annual rainfall mostly comes from its wet-season contribution based on satellite observations (Chavez & Takahashi, 2017). Therefore, the effects of Andean convection on Amazonian rainfall during austral summer are easier to detect than during other seasons. Second, it is during the wet season that CAM5, the atmospheric component of CESM, is known to produce the strongest rainfall deficit over southern Amazon (K. Zhang et al., 2017). Lastly, although the dry bias also exists during the dry season (June-July-Aug; JJA) in CESM v1, this is more likely to be caused by deficiencies in the land (Sakaguchi et al., 2018; K. Zhang et al., 2017), as opposed to the atmosphere component we are interested in. Similar to other CMIP6 models, the CESM v1.1 we used in our experiments has a similar WADA precipitation bias pattern during austral summer (Figure 1c,d).

2.2 Moisture budget analysis

2.2.1 Total advection of moisture

The local rate of change in specific humidity is calculated as

$$Q_t = \frac{QAP(t) - QAP(t-1)}{\delta t} \quad (2.1)$$

where QAP is the specific humidity after calculations of physics packages, δt is the time interval between two timestamps t and t-1.

The total advection of specific humidity is obtained by

$$Q_{adv} = Q_t - PTEQ \quad (2.2)$$

where PTEQ is the tendency of specific humidity calculated by physics packages at the corresponding time interval.

2.2.2 Decomposition in the total advection of moisture

On the other hand, the total advection of specific humidity can be estimated using gradient terms. The total advection of specific humidity can be written as

An edited version of this paper was published by AGU. Published (2025) American Geophysical Union.
Qin, H., Pritchard, M., Terai, C. R., Bacmeister, J., Bogenschutz, P., & Kiladis, G. N. (2025). Remote influence of Andean convection on Amazonian rainfall and its mechanisms. Journal of Geophysical Research: Atmospheres, 130, e2025JD043465. https://doi.org/10.1029/2025JD043465

$$-\boldsymbol{u}\frac{\partial \boldsymbol{q}}{\partial \boldsymbol{x}} - \boldsymbol{v}\frac{\partial \boldsymbol{q}}{\partial \boldsymbol{y}} - \boldsymbol{\omega}\frac{\partial \boldsymbol{q}}{\partial \boldsymbol{p}} \tag{2.3}$$

with the continuity equation

$$\frac{\partial \boldsymbol{u}}{\partial \boldsymbol{x}} + \frac{\partial \boldsymbol{v}}{\partial \boldsymbol{y}} + \frac{\partial \boldsymbol{\omega}}{\partial \boldsymbol{p}} = \boldsymbol{0} \tag{2.4}$$

the total advection of specific humidity can be written as

$$-\boldsymbol{u}\frac{\partial \boldsymbol{q}}{\partial \boldsymbol{x}} - \boldsymbol{v}\frac{\partial \boldsymbol{q}}{\partial \boldsymbol{y}} - \boldsymbol{\omega}\frac{\partial \boldsymbol{q}}{\partial \boldsymbol{p}} - \boldsymbol{q}\left(\frac{\partial \boldsymbol{u}}{\partial \boldsymbol{x}} + \frac{\partial \boldsymbol{v}}{\partial \boldsymbol{y}} + \frac{\partial \boldsymbol{\omega}}{\partial \boldsymbol{p}}\right)$$

or

$$-\left(\boldsymbol{u}\frac{\partial \boldsymbol{q}}{\partial \boldsymbol{x}} + \boldsymbol{v}\frac{\partial \boldsymbol{q}}{\partial \boldsymbol{y}}\right) - \boldsymbol{\omega}\frac{\partial \boldsymbol{q}}{\partial \boldsymbol{p}} - \boldsymbol{q}\left(\frac{\partial \boldsymbol{u}}{\partial \boldsymbol{x}} + \frac{\partial \boldsymbol{v}}{\partial \boldsymbol{y}}\right) - \boldsymbol{q}\frac{\partial \boldsymbol{\omega}}{\partial \boldsymbol{p}} \tag{2.5}$$

2.2.3 Differences of vertical moisture advection

The difference of the vertical advection of specific humidity between CTR and TOPO group can be written as

$$\langle -\boldsymbol{\omega}\frac{\partial \boldsymbol{q}}{\partial \boldsymbol{p}}\rangle_{\boldsymbol{CTR}} - \langle -\boldsymbol{\omega}\frac{\partial \boldsymbol{q}}{\partial \boldsymbol{p}}\rangle_{\boldsymbol{TOPO}}$$

or

$$\langle -\boldsymbol{\omega}\frac{\partial \boldsymbol{q}}{\partial \boldsymbol{p}}\rangle_{\boldsymbol{CTR-TOPO}} \tag{2.6}$$

where the brackets represent vertical integral. This term can be further decomposed into three terms (see Text S2) as follows

$$\langle -\boldsymbol{\omega}\frac{\partial \boldsymbol{q}}{\partial \boldsymbol{p}}\rangle_{\boldsymbol{CTR-TOPO}} = -\langle \boldsymbol{\omega}_{\boldsymbol{TOPO}}\left[\frac{\partial \boldsymbol{q}}{\partial \boldsymbol{p}}\right]_{\boldsymbol{CTR-TOPO}}\rangle - \langle \boldsymbol{\omega}_{\boldsymbol{CTR-TOPO}}\left[\frac{\partial \boldsymbol{q}}{\partial \boldsymbol{p}}\right]_{\boldsymbol{TOPO}}\rangle - \langle \boldsymbol{\omega}_{\boldsymbol{CTR-TOPO}}\left[\frac{\partial \boldsymbol{q}}{\partial \boldsymbol{p}}\right]_{\boldsymbol{CTR-TOPO}}\rangle \tag{2.7}$$

2.3 Other datasets

Besides model outputs of our sensitivity experiments, we also use Global Precipitation Climatology Project (GPCP) v2.3 (R. F. Adler et al., 2003; Robert F. Adler et al., 2018; G. J. Huffman et al., 2009), Tropical Rainfall Measuring Mission (TRMM) 3B42 dataset v7 (George J. Huffman et al., 2010), ERA5 Reanalysis (Hans et al., 2019; Hersbach et al., 2020), 39 models (Table S1) from the CMIP6 (Eyring et al., 2016; Z. Li et al., 2022) AMIP simulations, Atmospheric Infrared Sounder (AIRS) v7.0 (Kahn et al., 2014; B. Tian et al., 2020; B. J. Tian et al., 2013) datasets for auxiliary analysis.

An edited version of this paper was published by AGU. Published (2025) American Geophysical Union.
Qin, H., Pritchard, M., Terai, C. R., Bacmeister, J., Bogenschutz, P., & Kiladis, G. N. (2025). Remote influence of Andean convection on Amazonian rainfall and its mechanisms. Journal of Geophysical Research: Atmospheres, 130, e2025JD043465. https://doi.org/10.1029/2025JD043465

3 Responses of Amazonian rainfall to Andean convective heating

In this section, we first present baseline diurnal cycle features of precipitation in the control simulation and characteristics of Andean convective forcing in CESM, then demonstrate the effects of Andean convective forcing on non-local Amazonian rainfall, and finally test multiple hypotheses to understand the relevant processes and mechanisms.

3.1 Diurnal features of precipitation in the control simulation

Figure 3 presents the diurnal cycle phase and amplitude from the first harmonic of total precipitation in TRMM and CTR simulation during austral summer. TRMM depicts an early morning peak of precipitation over the ocean and a late-afternoon peak over land. Over the Amazon, TRMM clearly indicates late-afternoon peak in the diurnal cycle of precipitation, but convection occurs shortly after noon in the CTR simulation. This model bias is also seen in Cui et al. (2021) where this symptom can be alleviated by optimized deep convection triggering via using the dynamic convective available potential energy and the unrestricted launch level trigger (S. C. Xie et al., 2019). Admittedly, the diurnal cycle over the Amazon involves higher harmonics as well (Ruiz-Hernández et al., 2021).

3.2 Characteristics of Andean forcing

Figure 4 reviews the spatial and temporal structure of Andean convective forcing in the CTR group, which is necessary context for interpreting the consequences of its denial in the TOPO group. An equatorial (5°S-5°N) Hovmöller diagram (Figure 4a) of the composite diurnal rainfall cycle illustrates the afternoon maxima over the continental interior (east of 75°W) and nocturnal oceanic maxima (west of 75°W). A similar phenomenon has been noticed by Mapes et al. (2003) from satellite observations. The Andean forcing maximizes around local afternoon at 75°W (Figure 4a), and it exhibits a robust diurnal cycle approximately in phase with the diurnal cycle of rainfall in the CTR group. Its vertical structure reveals heating in the middle troposphere and cooling in the lower levels (Figure 4b). The horizontal structure of the vertically integrated Andean forcing (Figure 4c) shows decent alignment with Andean orography with peak net heating equatorward of 20°S (Figure 4c).

3.3 Responses of precipitation over the Amazon

In the following analysis, for physical interpretability, we will focus on the CTR-minus-TOPO anomalies since this can be regarded as a proxy for mechanisms associated with *including* the effects of Andean convective heating.

Our working hypothesis of remote control by Andean convection on Amazonian rainfall is confirmed, and its timescale is revealed in Figure 5c. During the 120 hours, the CTR group has five complete diurnal cycles with rainfall peaks reaching around 9 mm/day at local afternoon (Figure 5b). Comparing to TRMM, The CTR simulation has too early peaks of rainfall in its diurnal cycle (consistent with Figure 3) and the rainfall amount is severely underestimated. Amazonian precipitation is reduced as a response to Andean forcing in the first few days. and such reduction tapers off during nighttime after 48 hours (Figure 5c). Although the rainfall reduction maximum averaged over the Amazon box reaches around -1 mm/day, the reduction

An edited version of this paper was published by AGU. Published (2025) American Geophysical Union.
Qin, H., Pritchard, M., Terai, C. R., Bacmeister, J., Bogenschutz, P., & Kiladis, G. N. (2025). Remote influence of Andean convection on Amazonian rainfall and its mechanisms. Journal of Geophysical Research: Atmospheres, 130, e2025JD043465. https://doi.org/10.1029/2025JD043465

due to the Andean convection can reach 3 mm/day regionally (Figure 5a), which is comparable to the baseline wet-season dry bias in CESM (Figure 1c). The experiment setup and the short temporal scale Amazonian precipitation responses suggest that it is through fast atmospheric processes that such Andes–Amazon connection operates. As an aside, we note that local to the Andes, latent heat release enhances precipitation (Figure 5a, blue shading), which is expected since condensational heating can help strengthen a local convective cell (Holton, 2004). This answers our question raised in the introduction that parts of the WADA bias pattern can be at least partially driven from the Andes. Furthermore, after the first 2-3 days, the experiment suggests that internal variability of simulated atmosphere produces uncertainties as seen by the increasing spread in the simulations (Figure 5c) and the differences between CTR and TOPO experiments are indistinguishable from zero amongst 180 ensemble members (Figure S2). We will limit our analysis to the first 72 hours hereafter since this is when the experiment interference signals are not swamped by uncertainties and noise innate to atmospheric chaos (Lorenz, 1963).

3.4 Mechanisms of precipitation responses over the Amazon

In this section, we try to understand precipitation responses over the Amazon from the lenses of Convective Available Potential Energy (CAPE), the moisture budget, near-surface Moist Static Energy (MSE), and the mechanics of Gross Moist Stability (GMS).

Overall, based on the temporal evolution in precipitation responses over the Amazon, we find that the total advection of moisture provides a first-order control with a secondary impact from CAPE, while other mechanisms (e.g., MSE, GMS; Text S3, Text S4, Figure S3) are unable to explain the Amazonian precipitation changes.

First, we examine the role of CAPE. The deep convection scheme formulation is based on CAPE, the CTR-minus-TOPO precipitation response is dominated by convective component rather than large-scale component (Figure S4). In Figure 6d (also in Figure S5), there is significant reduction of CAPE over the Amazon after the 10th hour, especially during the 20th-60th hours, which suppresses deep convection and rainfall. This reduction of CAPE is linked to the boundary layer drying, which reduces dew point temperature and CAPE (Figure 6a latent static energy curve), as similarly mentioned in Langenbrunner et al. (2019). Nonetheless, this CAPE reduction is overall quite stable between 20th and 60th hour, a characteristic which is unable to explain near-zero response of Amazonian precipitation during 58-60th hours. On the other hand, the impact of Andean forcing on convective inhibition (CIN) is non-monotonic and it can not explain Amazonanian precipitation responses (Figure S6).

Next, we diagnose the moisture budget over the Amazon to show the dominant influence from the total advection of moisture. The local rate of change in moisture is balanced by moisture changes due to physics package calculations and the total advection of moisture (Figure 6c). In the CTR-minus-TOPO moisture budget (Figure 6c), during 1st-50th hours, 63th-70th hours, total advection of moisture decreases. During a similar period, precipitation also decreases and reaches a local minima (Figure 6h). However, during the 50th-63th hours, despite increases of total advection of moisture, precipitation is still moderately reduced over the Amazon except

An edited version of this paper was published by AGU. Published (2025) American Geophysical Union.
Qin, H., Pritchard, M., Terai, C. R., Bacmeister, J., Bogenschutz, P., & Kiladis, G. N. (2025). Remote influence of Andean convection on Amazonian rainfall and its mechanisms. Journal of Geophysical Research: Atmospheres, 130, e2025JD043465. https://doi.org/10.1029/2025JD043465

for a near-zero value around 58th-60th hours. This contradiction can be reconciled by considering the CAPE reduction. We speculate during 50th-63th hours, the effects of CAPE reduction dominate the effects of advective moistening on precipitation over the Amazon. As a result, rainfall is reduced despite the concurrent increase in total advection of moisture.

Furthermore, the vertical advective term drives the differences in the total advection of moisture. Based on (2.5), we decompose the total advection of specific humidity into four terms, the horizontal advective term $-\left(\boldsymbol{u}\frac{\partial \boldsymbol{q}}{\partial \boldsymbol{x}}+\boldsymbol{v}\frac{\partial \boldsymbol{q}}{\partial \boldsymbol{y}}\right)$, the divergence term $-\boldsymbol{q}\left(\frac{\partial \boldsymbol{u}}{\partial \boldsymbol{x}}+\frac{\partial \boldsymbol{v}}{\partial \boldsymbol{y}}\right)$, the vertical advective term $-\boldsymbol{\omega}\frac{\partial \boldsymbol{q}}{\partial \boldsymbol{p}}$, and the vertical Omega gradient term$-\boldsymbol{q}\frac{\partial \boldsymbol{\omega}}{\partial \boldsymbol{p}}$. This decomposition is shown in Figure 6e. Please be aware that this way of calculating total advection on model outputs is prone to be erroneous and needs to be carefully handled (e.g., to avoid unnecessary vertical interpolation from hybrid to pressure coordinates, we use spherical harmonics to estimate gradients). For validation and comparison, the more accurate moisture total advection calculation based on (2.1) and (2.2) are shown in Figure 6f. The resemblance of the total advection curves based on these two methods in Figure 6f justifies the decomposition results calculated using gradient terms. On one hand, the divergence term (yellow) is always in balance with the vertical Omega gradient term (red) due to the continuity equation (2.4). On the other hand, the horizontal advective term (blue) is negligible compared to the other terms. Therefore, the total advection as the sum of the four components is mostly determined by the vertical advective term $-\boldsymbol{\omega}\frac{\partial \boldsymbol{q}}{\partial \boldsymbol{p}}$.

Moreover, differences in the vertical advective term between CTR and TOPO are mainly driven by differences in the vertical velocity field. The vertical advective term difference between CTR and TOPO group $\langle-\boldsymbol{\omega}\frac{\partial \boldsymbol{q}}{\partial \boldsymbol{p}}\rangle_{\boldsymbol{CTR-TOPO}}$(blue curve in Figure 6g) can be decomposed via equation (2.7) into $-\langle\boldsymbol{\omega}_{\boldsymbol{TOPO}}\left[\frac{\partial \boldsymbol{q}}{\partial \boldsymbol{p}}\right]_{\boldsymbol{CTR-TOPO}}\rangle$ (yellow curve), $-\langle\boldsymbol{\omega}_{\boldsymbol{CTR-TOPO}}\left[\frac{\partial \boldsymbol{q}}{\partial \boldsymbol{p}}\right]_{\boldsymbol{TOPO}}\rangle$ (green curve), and $-\langle\boldsymbol{\omega}_{\boldsymbol{CTR-TOPO}}\left[\frac{\partial \boldsymbol{q}}{\partial \boldsymbol{p}}\right]_{\boldsymbol{CTR-TOPO}}\rangle$ (red curve). The differences of the vertical advective term $\langle-\boldsymbol{\omega}\frac{\partial \boldsymbol{q}}{\partial \boldsymbol{p}}\rangle_{\boldsymbol{CTR-TOPO}}$ is driven by $-\langle\boldsymbol{\omega}_{\boldsymbol{CTR-TOPO}}\left[\frac{\partial \boldsymbol{q}}{\partial \boldsymbol{p}}\right]_{\boldsymbol{TOPO}}\rangle$, or differences of vertical velocity field between CTR and TOPO group, revealing the importance of the vertical dynamic field. In addition, the vertical gradient of specific humidiy in the TOPO group also plays a role.

The moisture distribution decreases with height in the TOPO group (Figure S7), it is a positive term in pressure coordinate. There are descending anomalies over the Amazon in the CTR-minus-TOPO (see section 4), which leads to positive $\boldsymbol{\omega}_{\boldsymbol{CTR-TOPO}}$. Therefore, the total effect is negative in this term $-\langle\boldsymbol{\omega}_{\boldsymbol{CTR-TOPO}}\left[\frac{\partial \boldsymbol{q}}{\partial \boldsymbol{p}}\right]_{\boldsymbol{TOPO}}\rangle$, meaning stronger descending anomalies bring negative vertical moisture advection that reduces humidity in free troposphere and boundary layer. The entrainment drying effect at the boundary layer is reflected by the reduced lower-level latent static energy $\boldsymbol{L_v q}$ as shown in Figure 6a. Over the Amazon, the descending anomalies also reduce cloud fraction above 600hPa (Figure 7), leading to increase of shortwave

An edited version of this paper was published by AGU. Published (2025) American Geophysical Union.
Qin, H., Pritchard, M., Terai, C. R., Bacmeister, J., Bogenschutz, P., & Kiladis, G. N. (2025). Remote influence of Andean convection on Amazonian rainfall and its mechanisms. Journal of Geophysical Research: Atmospheres, 130, e2025JD043465. https://doi.org/10.1029/2025JD043465

cloud forcing (Figure S8). As a result, the surface net radiation increases in CTR-minus-TOPO driven by the elevated shortwave component (Figure S9).

In summary, the Amazonian precipitation responses can be explained by (a) differences of moisture vertical advection term $\langle -\boldsymbol{\omega}\frac{\partial \boldsymbol{q}}{\partial \boldsymbol{p}}\rangle_{\boldsymbol{CTR-TOPO}}$ driven by $-\langle \boldsymbol{\omega}_{\boldsymbol{CTR-TOPO}}\left[\frac{\partial \boldsymbol{q}}{\partial \boldsymbol{p}}\right]_{\boldsymbol{TOPO}}\rangle$, and (b) modulation of CAPE differences between CTR and TOPO.

4 Eastward expansion features

In section 3.4, we have shown that the vertical advective term $\langle -\boldsymbol{\omega}\frac{\partial \boldsymbol{q}}{\partial \boldsymbol{p}}\rangle_{\boldsymbol{CTR-TOPO}}$ is a first-order control on reductions of the total advection of moisture that is in turn implicated via its timescale of onset with the precipitation changes of interest. This view is corroborated when we examine a 10°S latitude transect (Figure 8). Initially, only on the east flank of the Andes can the strong subsidence anomalies be found. Then, the horizontal scale of the sinking anomalies expands eastward progressively (Figure 8a-d) with a concurring expansion of drying in the troposphere (Figure 8e-h). Consistently, in the middle troposphere, the vertical velocity anomalies gradually progress eastward during the 4-11th hours with the subsequent eastward stride of reduced specific humidity with a few hours lag (Figure S10). The eastward propogation feature with 850hPa geopotential height is related to Kelvin waves (Figure 9).

In Figure 8, we see there vertical motion and humidity dipoles in the lowermost troposphere over the Andes. We think that the CTR-minus-TOPO distills the effect of condensational heating (upper troposphere, warmer temperature in Figure 8a-d) and re-evaporative cooling (lower troposphere, cooler temperature in Figure 8a-d). In Figure 8, at hour 4 and 7, the vertical winds are upward anomalies in those blue blobs. At later hours (10, 13), there are descending anomalies in those blue blobs which might be caused by cooling. In the humidity dipole in Figure 8f-h, the CTR has massive precipitation occurring over the Andes (likely implies a close-to-saturated troposphere), and the temperature tendency changes lead to a more (less) humid environment with warming (cooling) temperature tendencies dictated by the Clausius-Clapeyron relationship under saturated conditions. Furthermore, the increase of humidity in the near-surface level can result from precipitation and re-evaporation, while the reduction of humidity near 700mb and increase above may be due to enhanced vertical transport of moisture by parameterized convection and resolved transport in CTR simulation.

5 Discussion

Our experiment setup leads to enhanced SALLJ in CTR compared with TOPO (Figure 10), the resulting elevated Andean precipitation and suppressed rainfall over Amazon seems consistent with findings in ancient climate by Vizy and Cook (2007). Interestingly, we can weaken the LLJ by denying the latent heat release from convection activities over the Andes, which is similar to lowering the Andean topography as shown in earlier studies (Insel et al., 2010; Rasmussen & Houze, 2016). Figure S11 also indicates that Andean convective forcing can cause weakened moisture flux convergence over the Amazon.

An edited version of this paper was published by AGU. Published (2025) American Geophysical Union.
Qin, H., Pritchard, M., Terai, C. R., Bacmeister, J., Bogenschutz, P., & Kiladis, G. N. (2025). Remote influence of Andean convection on Amazonian rainfall and its mechanisms. Journal of Geophysical Research: Atmospheres, 130, e2025JD043465. https://doi.org/10.1029/2025JD043465

Moreover, we expect the Andean-driven contribution will vary for different models. It could be non-trivial for some models but not for others. From the CMIP6 model analysis, preliminary evidence implies that the Andean driven contribution is likely to be non-dominant when all 39 models are considered given the absence of negative correlation between Andean precipitation bias and Amazonian precipitation bias (Figure S12).

Regarding the resolution dependence of our results, we noticed that in Hsi-Yen Ma et al. (2021), CAM5 on 0.9°x1.25° grids also show this WADA bias pattern. While our results are based on nominal 2-degree grids, we don't expect the results to change qualitatively since the root cause of errors in calculating pressure gradient force is inherently borne out of the "dynamics" near steep topographies which also exists in 0.9°x1.25° grids. In another evaluation study of the atmospheric component of the Energy Exascale Earth System Model (E3SM) v1 (Golaz et al., 2019), the dipole pattern of precipitation bias along elevated terrains (e.g., Wet Andes and Dry Amazon, Wet Rockies and Dry central US, Wet Himalayas and Dry Bangladesh) is present in both the standard resolution (Δx = 110km) and high-resolution (Δx = 25km) and thus is a robust feature which is not alleviated due to higher resolution (Caldwell et al., 2019). Following the E3SM lineage, improved precipitation over Amazon is found with a global cloud-resolving atmospheric model SCREAM (Caldwell et al., 2021) at 3.25km horizontal resolution likely due to better resolved convection and more realistic topography. The WADA bias pattern exists not only in E3SM v1 but also in its version 2 as seen in Figure 13 in Golaz et al. (2022). By using optimized deep convection triggering via dynamic convective available potential energy and unrestricted launch level trigger, the diurnal cycle and dry bias of precipitation over the Amazon can be improved in both E3SM (S. Xie et al., 2019) and CAM5 (Cui et al., 2021).

6 Summary and conclusion

Motivated by the systematic WADA precipitation bias pattern seen in the CMIP6 archive over tropical South America, we design mechanism denial experiments to surgically isolate the effects of Andean convective forcing on Amazonian precipitation processes. Based on an ensemble hindcast approach, we illustrate that Amazonian precipitation is notably reduced within hours after initial Andean convective forcing, and examine its causality. The magnitude of rainfall reduction over certain parts of the Amazon can reach beyond 3 mm/day, which is comparable to the magnitude of CMIP6 rainfall deficit biases during wet-season. The precipitation decrease over the Amazon is primarily controlled by the total advection of moisture driven by the vertical advective term $-\omega\frac{\partial q}{\partial p}$ and is also affected by local CAPE reduction. Differences in the vertical advective term between CTR and TOPO group $\langle -\omega\frac{\partial q}{\partial p}\rangle_{CTR-TOPO}$ are traced to differences of vertical velocity between two groups. In a nutshell, the evidence suggests that heating from Andean convection initially induces strong subsidence anomalies on its east flank, which then gradually expands eastward towards the Amazon basin which is linked to Kelvin waves. As a consequence of vertical advective term, a similar eastward expansion of tropospheric drying is easily visible and detectable on a similar horizontal length scale. In CTR-minus-TOPO, the stronger descending anomalies bring negative vertical moisture advection that reduces humidity in free troposphere and boundary layer. This

An edited version of this paper was published by AGU. Published (2025) American Geophysical Union.
Qin, H., Pritchard, M., Terai, C. R., Bacmeister, J., Bogenschutz, P., & Kiladis, G. N. (2025). Remote influence of Andean convection on Amazonian rainfall and its mechanisms. Journal of Geophysical Research: Atmospheres, 130, e2025JD043465. https://doi.org/10.1029/2025JD043465

leads to reduced mid-to-high level cloud and increased thermodynamic stability over the Amazon.

Another question to answer is how much dry precipitation bias over the Amazon can be explained by the Andean-driven mechanisms as opposed to other error sources such as atmospheric convection parameterization, land processes, oceanic influence. One possible route to address this question is to apply 20%, 40%, 60%, 80%, and 100% of the temperature tendency denial and examine if the Amazonian response shows linear behaviors to the magnitude of Andean forcing. If confirmed, the Andean wet-bias equivalent of convective heating can be proportionally translated into precipitation reduction response over the Amazon. We can then divide such precipitation reduction by the total rainfall dry bias over the Amazon. This will give an estimate about how much Amazonian precipitation dry bias is contributed by the Andean-driven mechanism. Another approach is to design heating tendency denial along the Andes with magnitude comparable to the Andean precipitation wet bias as opposed to the full-denial in the current experiment set-up. These two approaches are potential avenues for follow-up research.

There is caveat on the mechanism-denial experiments. The purpose in designing this experiment is to causatively determine the effects of Andean convective forcing on Amazonian rainfall. To achieve this, we first have a full-fledged CTR group simulation, and then have a second TOPO group in which we numerically mute the convective forcing over mountainous terrains. By comparing these two groups of simulations, we can seperate the effects of Andean convective forcing on Amazonian rainfall. The tradeoff of such experiment design is the violation of energy conservation. Simulations in the second TOPO group allow precipitation to occur but disallow latent heat release from condensation over Andean topography. The interference in the TOPO group inevitably means the annihilation of the latent heat energy encapsulated in precipitation. We readily admit that our idealized mechanim denial experiments are simply a pragmatic way to probe the system's feedbacks to identify how Amazonian rainfall responds to the latent heat release from Andean convection and how the system adapts to such disturbances, whose results are beneficial to gain insights about the dynamics within the system despite such imperfections in experiment design. Indeed, we focus on the first few days in our analysis, during which the disturbances should be primarily driven by local Andean latent heating, and the effect of energy conservation violation is presumably limited. Another caveat is that our experiments were run using an older version of CESM. Although we do not expect the main results to change qualitatively in newer version of the model, the magnitude of the Andean-driven Amazonian response might differ slightly.

Despite aforementioned limitations, our study is enlightening in the following aspects.

First, our results confirm a previously underappreciated effect of remote Andean control on Amazonian precipitation at weather timescale. The weather timescale of Andean driven Amazonian precipitation responses provides complementary insights to the hindcast approach in developing and improving convection parameterizations (H.-Y. Ma et al., 2015; H.-Y. Ma et al., 2013; Phillips et al., 2004). The hindcast idea is realistically initializing climate models with

An edited version of this paper was published by AGU. Published (2025) American Geophysical Union.
Qin, H., Pritchard, M., Terai, C. R., Bacmeister, J., Bogenschutz, P., & Kiladis, G. N. (2025). Remote influence of Andean convection on Amazonian rainfall and its mechanisms. Journal of Geophysical Research: Atmospheres, 130, e2025JD043465. https://doi.org/10.1029/2025JD043465

numerical weather prediction analyses or reanalyzes data, during the short hindcast period within a few days, the large-scale state is still close to observations and thus the model biases in clouds and convection processes are largely attributed to errors in parameterizations. As a result, lessons learned from climate model hindcasts could help aid convection parameterization developements. Our present study illustrates that over tropical South America, part of precipitation biases on such short timescale comes from the "dynamics" part in the model, which is likely associated with pressure gradient force errors inherited from dynamic solvers near steep topographies rather than parameterized "physics". Efforts to improve cloud parameterizations will certainly be helpful to relieve the precipitation bias over the Amazon. However, our results imply that improvement in cloud parameterizations alone is insufficient to eliminate the precipitation bias over the Andes-Amazon region.

Second, our sensitivity experiment emphasizes the role of mid-tropospheric vertical velocity and moisture field for the Andean convective forcing to exert influence on Amazonian rainfall. For model evaluators who are keen on Amazonian hydroclimate, we suggest incorporations of Andean east flank dynamical and moisture field into their model evaluation strategy.

Finally, our study underscores the importance of looking at the Andes-Amazon holistically, and the Andes-Amazon ought to be assessed together in climate change studies. In a warmer climate, Amazonia is projected to experience decrease of rainfall (Pascale et al., 2019), a strengthening and lengthened dry season (Joetzjer et al., 2013), more frequent and exacerbated meteorological droughts (Duffy et al., 2015). Our sensitivity study suggests that future changes of Andean convection and precipitation may influence Amazonian hydroclimate through intricate feedbacks. For instance, a decrease or increase of Andean rainfall in the future (Neukom et al., 2015; Seiler et al., 2013; Urrutia & Vuille, 2009) might alleviate or exacerbate the rainfall deficits over the Amazon. Missing the Andean component in Amazonian hydroclimate projections in the future will weaken the reliability of local mitigation and adaptation strategies.

Acknowledgments

This work is supported by Department of Energy grant DE-SC0012152. We acknowledge computational support from the Extreme Science and Engineering Discovery Environment under allocation TG-ATM120034. Work by CRT and PB were conducted under the auspices of the DOE by Lawrence Livermore National Laboratory under Contract DE-AC52-07NA27344.
LLNL-JRNL-2015082

Open Research

An edited version of this paper was published by AGU. Published (2025) American Geophysical Union.
Qin, H., Pritchard, M., Terai, C. R., Bacmeister, J., Bogenschutz, P., & Kiladis, G. N. (2025). Remote influence of Andean convection on Amazonian rainfall and its mechanisms. Journal of Geophysical Research: Atmospheres, 130, e2025JD043465. https://doi.org/10.1029/2025JD043465

Simulation outputs from control and experiment groups are accessible via NERSC Science Gateway portal (WADA, 2024). Global Precipitation Climatology Project (GPCP) version 2.3 is available at Adler et al. (2018). Tropical Rainfall Measuring Mission (TRMM) 3B42 dataset version 7 is available at Huffman et al. (2010). ERA5 Reanalysis is available at Hersbach et al. (2020). CMIP6 AMIP simulations are available at ESGF (2024). Atmospheric Infrared Sounder (AIRS) version 7.0 is available at Tian et al. (2020).

References

WADA (2024), numerical simulations in the WADA project via NERSC Science Gateway portal [Dataset]. https://portal.nersc.gov/archive/home/h/hongcheq/www/WADA

Adler et al. (2018), GPCP v2.3, NOAA Physical Sciences Laboratory [Dataset]. https://psl.noaa.gov/data/gridded/data.gpcp.html

Huffman et al. (2010), TRMM 3B42, NASA Earth Data [Dataset]. https://disc.gsfc.nasa.gov/datasets/TRMM_3B42_7/summary?keywords=TRMM_3B42

Hersbach et al. (2020), ERA5 Reanalysis, ECMWF [Dataset]. https://cds.climate.copernicus.eu/datasets/reanalysis-era5-complete?tab=overview

ESGF. (2024) , CMIP6 AMIP, Earth System Grid Federation [Dataset]. https://aims2.llnl.gov/search/cmip6

Tian et al. (2020), Atmospheric Infrared Sounder (AIRS) v7.0, NASA Earth Data [Dataset]. https://disc.gsfc.nasa.gov/datasets/AIRS3STM_7.0/summary?keywords=airs%20version%207

Eyring, V., N.P. Gillett, K.M. Achuta Rao, R. Barimalala, M. Barreiro Parrillo, N. Bellouin, C. Cassou, P.J. Durack, Y. Kosaka, S. McGregor, S. Min, O. Morgenstern, and Y. Sun, 2021: Human Influence on the Climate System. In Climate Change 2021: The Physical Science Basis. Contribution of Working Group I to the Sixth Assessment Report of the Intergovernmental Panel on Climate Change [Masson-Delmotte, V., P. Zhai, A. Pirani, S.L. Connors, C. Péan, S. Berger, N. Caud, Y. Chen, L. Goldfarb, M.I. Gomis, M. Huang, K. Leitzell, E. Lonnoy, J.B.R. Matthews, T.K. Maycock, T. Waterfield, O. Yelekçi, R. Yu, and B. Zhou (eds.)]. Cambridge University Press, Cambridge, United Kingdom and New York, NY, USA, pp. 423–552, doi: 10.1017/9781009157896.005.

Adler, R. F., Huffman, G. J., Chang, A., Ferraro, R., Xie, P. P., Janowiak, J., et al. (2003). The version-2 global precipitation climatology project (GPCP) monthly precipitation analysis (1979-present). *Journal of Hydrometeorology, 4*(6), 1147-1167. <Go to ISI>://WOS:000187534900011

Adler, R. F., Sapiano, M. R. P., Huffman, G. J., Wang, J.-J., Gu, G., Bolvin, D., et al. (2018). The Global Precipitation Climatology Project (GPCP) Monthly Analysis (New Version 2.3) and a Review of 2017 Global Precipitation. *Atmosphere, 9*(4). Retrieved from doi:10.3390/atmos9040138

Anber, U., Gentine, P., Wang, S., & Sobel, A. H. (2015). Fog and rain in the Amazon. *Proc Natl Acad Sci U S A, 112*(37), 11473-11477. https://www.ncbi.nlm.nih.gov/pubmed/26324902

Avissar, R., & Werth, D. (2005). Global hydroclimatological teleconnections resulting from tropical deforestation. *Journal of Hydrometeorology, 6*(2), 134-145. <Go to ISI>://WOS:000228975200003

Baker, J. C. A., & Spracklen, D. V. (2022). Divergent Representation of Precipitation Recycling in the Amazon and the Congo in CMIP6 Models. *Geophysical Research Letters, 49*(10), e2021GL095136. https://agupubs.onlinelibrary.wiley.com/doi/abs/10.1029/2021GL095136

Barros, V. R., & Doyle, M. E. (2018). Low-level circulation and precipitation simulated by CMIP5 GCMS over southeastern South America. *International Journal of Climatology, 38*(15), 5476-5490. https://rmets.onlinelibrary.wiley.com/doi/abs/10.1002/joc.5740

Boers, N., Marwan, N., Barbosa, H. M., & Kurths, J. (2017). A deforestation-induced tipping point for the South American monsoon system. *Sci Rep, 7*, 41489. https://www.ncbi.nlm.nih.gov/pubmed/28120928

Caldwell, P. M., Mametjanov, A., Tang, Q., Van Roekel, L. P., Golaz, J.-C., Lin, W., et al. (2019). The DOE E3SM Coupled Model Version 1: Description and Results at High Resolution. *Journal of Advances in Modeling Earth Systems, 11*(12), 4095-4146. https://agupubs.onlinelibrary.wiley.com/doi/abs/10.1029/2019MS001870

Caldwell, P. M., Terai, C. R., Hillman, B., Keen, N. D., Bogenschutz, P., Lin, W., et al. (2021). Convection-Permitting Simulations With the E3SM Global Atmosphere Model. *Journal of Advances in Modeling Earth*

An edited version of this paper was published by AGU. Published (2025) American Geophysical Union.
Qin, H., Pritchard, M., Terai, C. R., Bacmeister, J., Bogenschutz, P., & Kiladis, G. N. (2025). Remote influence of Andean convection on Amazonian rainfall and its mechanisms. Journal of Geophysical Research: Atmospheres, 130, e2025JD043465. https://doi.org/10.1029/2025JD043465

Systems, 13(11), e2021MS002544. https://agupubs.onlinelibrary.wiley.com/doi/abs/10.1029/2021MS002544

Chavez, S. P., & Takahashi, K. (2017). Orographic rainfall hot spots in the Andes-Amazon transition according to the TRMM precipitation radar and in situ data. *Journal of Geophysical Research: Atmospheres, 122*(11), 5870-5882. https://agupubs.onlinelibrary.wiley.com/doi/abs/10.1002/2016JD026282 https://agupubs.onlinelibrary.wiley.com/doi/pdf/10.1002/2016JD026282

Chen, Y., Langenbrunner, B., & Randerson, J. T. (2018). Future Drying in Central America and Northern South America Linked With Atlantic Meridional Overturning Circulation. *Geophysical Research Letters, 45*(17), 9226-9235. <Go to ISI>://WOS:000445727500058 https://agupubs.onlinelibrary.wiley.com/doi/full/10.1029/2018GL077953

Cui, Z., Zhang, G. J., Wang, Y., & Xie, S. (2021). Understanding the Roles of Convective Trigger Functions in the Diurnal Cycle of Precipitation in the NCAR CAM5. *Journal of Climate, 34*(15), 6473-6489. https://journals.ametsoc.org/view/journals/clim/34/15/JCLI-D-20-0699.1.xml https://journals.ametsoc.org/downloadpdf/view/journals/clim/34/15/JCLI-D-20-0699.1.pdf

Duffy, P. B., Brando, P., Asner, G. P., & Field, C. B. (2015). Projections of future meteorological drought and wet periods in the Amazon. *Proceedings of the National Academy of Sciences of the United States of America, 112*(43), 13172-13177. <Go to ISI>://WOS:000363458100035 https://www.ncbi.nlm.nih.gov/pmc/articles/PMC4629378/pdf/pnas.201421010.pdf

Eyring, V., Bony, S., Meehl, G. A., Senior, C. A., Stevens, B., Stouffer, R. J., & Taylor, K. E. (2016). Overview of the Coupled Model Intercomparison Project Phase 6 (CMIP6) experimental design and organization. *Geosci. Model Dev., 9*(5), 1937-1958. https://gmd.copernicus.org/articles/9/1937/2016/

Fernandes, K., Giannini, A., Verchot, L., Baethgen, W., & Pinedo-Vasquez, M. (2015). Decadal covariability of Atlantic SSTs and western Amazon dry-season hydroclimate in observations and CMIP5 simulations. *Geophysical Research Letters, 42*(16), 6793-6801. <Go to ISI>://WOS:000363410800034

Gettelman, A., Hegglin, M. I., Son, S. W., Kim, J., Fujiwara, M., Birner, T., et al. (2010). Multimodel assessment of the upper troposphere and lower stratosphere: Tropics and global trends. *JOURNAL OF GEOPHYSICAL RESEARCH-ATMOSPHERES, 115*. <Go to ISI>://WOS:000283546600002

Golaz, J.-C., Caldwell, P. M., Van Roekel, L. P., Petersen, M. R., Tang, Q., Wolfe, J. D., et al. (2019). The DOE E3SM Coupled Model Version 1: Overview and Evaluation at Standard Resolution. *Journal of Advances in Modeling Earth Systems, 11*(7), 2089-2129. https://agupubs.onlinelibrary.wiley.com/doi/abs/10.1029/2018MS001603

Golaz, J.-C., Van Roekel, L. P., Zheng, X., Roberts, A. F., Wolfe, J. D., Lin, W., et al. (2022). The DOE E3SM Model Version 2: Overview of the Physical Model and Initial Model Evaluation. *Journal of Advances in Modeling Earth Systems, 14*(12), e2022MS003156. https://agupubs.onlinelibrary.wiley.com/doi/abs/10.1029/2022MS003156

Hans, H., Bell, W., Berrisford, P., Andras, H., Muñoz-Sabater, J., Nicolas, J., et al. (2019). Global reanalysis: goodbye ERA-Interim, hello ERA5. *ECMWF Newsletter*.

Hersbach, H., Bell, B., Berrisford, P., Hirahara, S., Horányi, A., Muñoz-Sabater, J., et al. (2020). The ERA5 global reanalysis. *Quarterly Journal of the Royal Meteorological Society, 146*(730), 1999-2049. https://doi.org/10.1002/qj.3803

Holton, J. R. (2004). *An introduction to dynamic meteorology* (4th ed.). Burlington, MA: Elsevier Academic Press.

Huffman, G. J., Adler, R. F., Bolvin, D. T., & Gu, G. J. (2009). Improving the global precipitation record: GPCP Version 2.1. *Geophysical Research Letters, 36*(17), L17808-L17808. <Go to ISI>://WOS:000269756100006

Huffman, G. J., Adler, R. F., Bolvin, D. T., & Nelkin, E. J. (2010). The TRMM Multi-Satellite Precipitation Analysis (TMPA). In M. Gebremichael & F. Hossain (Eds.), *Satellite Rainfall Applications for Surface Hydrology* (pp. 3-22). Dordrecht: Springer Netherlands.

Iacono, M. J., Delamere, J. S., Mlawer, E. J., Shephard, M. W., Clough, S. A., & Collins, W. D. (2008). Radiative forcing by long-lived greenhouse gases: Calculations with the AER radiative transfer models. *JOURNAL OF GEOPHYSICAL RESEARCH-ATMOSPHERES, 113*(D13). <Go to ISI>://WOS:000257431600004

Insel, N., Poulsen, C. J., & Ehlers, T. A. (2010). Influence of the Andes Mountains on South American moisture transport, convection, and precipitation. *Climate Dynamics, 35*(7-8), 1477-1492. journal article. <Go to ISI>://WOS:000284483800020

IPCC. (2014). Evaluation of Climate Models. In T. F. Stocker, D. Qin, G.-K. Plattner, M. Tignor, S. K. Allen, J. Boschung, A. Nauels, Y. Xia, V. Bex, & P. M. Midgley (Eds.), *Climate Change 2013 - The Physical*

An edited version of this paper was published by AGU. Published (2025) American Geophysical Union.
Qin, H., Pritchard, M., Terai, C. R., Bacmeister, J., Bogenschutz, P., & Kiladis, G. N. (2025). Remote influence of Andean convection on Amazonian rainfall and its mechanisms. Journal of Geophysical Research: Atmospheres, 130, e2025JD043465. https://doi.org/10.1029/2025JD043465

Science Basis (pp. 741-866). Cambridge, United Kingdom and New York, NY, USA: Cambridge University Press.

Joetzjer, E., Douville, H., Delire, C., & Ciais, P. (2013). Present-day and future Amazonian precipitation in global climate models: CMIP5 versus CMIP3. *Climate Dynamics, 41*(11-12), 2921-2936. <Go to ISI>://WOS:000327080400008

Kahn, B. H., Irion, F. W., Dang, V. T., Manning, E. M., Nasiri, S. L., Naud, C. M., et al. (2014). The Atmospheric Infrared Sounder version 6 cloud products. *Atmos. Chem. Phys., 14*(1), 399-426. https://acp.copernicus.org/articles/14/399/2014/

Kooperman, G. J., Chen, Y., Hoffman, F. M., Koven, C. D., Lindsay, K., Pritchard, M. S., et al. (2018). Forest response to rising CO2 drives zonally asymmetric rainfall change over tropical land. *Nature Climate Change, 8*(5), 434-+. <Go to ISI>://WOS:000431139900028

Langenbrunner, B., Pritchard, M. S., Kooperman, G. J., & Randerson, J. T. (2019). Why Does Amazon Precipitation Decrease When Tropical Forests Respond to Increasing CO2? *Earths Future, 7*(4), 450-468. <Go to ISI>://WOS:000467396900010

https://agupubs.onlinelibrary.wiley.com/doi/full/10.1029/2018EF001026

Lawrence, D., & Vandecar, K. (2015). Effects of tropical deforestation on climate and agriculture. *Nature Climate Change, 5*(2), 174-174. <Go to ISI>://WOS:000350327700031

Li, L. H., Wang, Y. P., Arora, V. K., Eamus, D., Shi, H., Li, J., et al. (2018). Evaluating Global Land Surface Models in CMIP5: Analysis of Ecosystem Water- and Light-Use Efficiencies and Rainfall Partitioning. *Journal of Climate, 31*(8), 2995-3008. <Go to ISI>://WOS:000428694000002

Li, Z., Liu, T., Huang, Y., Peng, J., & Ling, Y. (2022). Evaluation of the CMIP6 Precipitation Simulations Over Global Land. *Earth's Future, 10*(8), e2021EF002500. https://agupubs.onlinelibrary.wiley.com/doi/abs/10.1029/2021EF002500

Lintner, B. R., Adams, D. K., Schiro, K. A., Stansfield, A. M., Rocha, A. A. A., & Neelin, J. D. (2017). Relationships among climatological vertical moisture structure, column water vapor, and precipitation over the central Amazon in observations and CMIP5 models. *Geophysical Research Letters, 44*(4), 1981-1989. <Go to ISI>://WOS:000396411100044

Lorenz, E. N. (1963). Deterministic Nonperiodic Flow. *Journal of Atmospheric Sciences, 20*(2), 130-141. https://journals.ametsoc.org/view/journals/atsc/20/2/1520-0469_1963_020_0130_dnf_2_0_co_2.xml

Ma, H.-Y., Chuang, C. C., Klein, S. A., Lo, M.-H., Zhang, Y., Xie, S., et al. (2015). An improved hindcast approach for evaluation and diagnosis of physical processes in global climate models. *Journal of Advances in Modeling Earth Systems, 7*(4), 1810-1827. https://agupubs.onlinelibrary.wiley.com/doi/abs/10.1002/2015MS000490

Ma, H.-Y., Xie, S., Boyle, J. S., Klein, S. A., & Zhang, Y. (2013). Metrics and Diagnostics for Precipitation-Related Processes in Climate Model Short-Range Hindcasts. *Journal of Climate, 26*(5), 1516-1534. https://journals.ametsoc.org/view/journals/clim/26/5/jcli-d-12-00235.1.xml

Ma, H.-Y., Zhang, K., Tang, S., Xie, S., & Fu, R. (2021). Evaluation of the Causes of Wet-Season Dry Biases Over Amazonia in CAM5. *Journal of Geophysical Research: Atmospheres, 126*(11), e2020JD033859. https://agupubs.onlinelibrary.wiley.com/doi/abs/10.1029/2020JD033859

https://agupubs.onlinelibrary.wiley.com/doi/pdfdirect/10.1029/2020JD033859?download=true

Mapes, B. E., Warner, T. T., Xu, M., & Negri, A. J. (2003). Diurnal patterns of rainfall in northwestern South America. Part I: Observations and context. *Monthly Weather Review, 131*(5), 799-812. <Go to ISI>://WOS:000182172000004

Medvigy, D., Walko, R. L., Otte, M. J., & Avissar, R. (2013). Simulated Changes in Northwest US Climate in Response to Amazon Deforestation. *Journal of Climate, 26*(22), 9115-9136. <Go to ISI>://WOS:000326216500024

Meehl, G. A., Shields, C., Arblaster, J. M., Annamalai, H., & Neale, R. (2020). Intraseasonal, Seasonal, and Interannual Characteristics of Regional Monsoon Simulations in CESM2. *Journal of Advances in Modeling Earth Systems, 12*(6), e2019MS001962. https://agupubs.onlinelibrary.wiley.com/doi/abs/10.1029/2019MS001962

Mehran, A., AghaKouchak, A., & Phillips, T. J. (2014). Evaluation of CMIP5 continental precipitation simulations relative to satellite- based gauge- adjusted observations. *JOURNAL OF GEOPHYSICAL RESEARCH-ATMOSPHERES, 119*(4), 1695-1707. <Go to ISI>://WOS:000333138300001

Mlawer, E. J., Taubman, S. J., Brown, P. D., Iacono, M. J., & Clough, S. A. (1997). Radiative transfer for inhomogeneous atmospheres: RRTM, a validated correlated-k model for the longwave. *JOURNAL OF*

GEOPHYSICAL RESEARCH-ATMOSPHERES, 102(D14), 16663-16682. <Go to ISI>://WOS:A1997XN38400019

Morrison, H., & Gettelman, A. (2008). A new two-moment bulk stratiform cloud microphysics scheme in the community atmosphere model, version 3 (CAM3). Part I: Description and numerical tests. *Journal of Climate, 21*(15), 3642-3659. <Go to ISI>://WOS:000258190100002

Mueller, B., & Seneviratne, S. I. (2014). Systematic land climate and evapotranspiration biases in CMIP5 simulations. *Geophys Res Lett, 41*(1), 128-134. https://www.ncbi.nlm.nih.gov/pubmed/26074635

Neukom, R., Rohrer, M., Calanca, P., Salzmann, N., Huggel, C., Acuña, D., et al. (2015). Facing unprecedented drying of the Central Andes? Precipitation variability over the period AD 1000–2100. *Environmental Research Letters, 10*(8), 084017. http://dx.doi.org/10.1088/1748-9326/10/8/084017

Park, S., & Bretherton, C. S. (2009). The University of Washington Shallow Convection and Moist Turbulence Schemes and Their Impact on Climate Simulations with the Community Atmosphere Model. *Journal of Climate, 22*(12), 3449-3469. <Go to ISI>://WOS:000268126300016

Park, S., Bretherton, C. S., & Rasch, P. J. (2014). Integrating Cloud Processes in the Community Atmosphere Model, Version 5. *Journal of Climate, 27*(18), 6821-6856. <Go to ISI>://WOS:000341981800001

Pascale, S., Carvalho, L. M. V., Adams, D. K., Castro, C. L., & Cavalcanti, I. F. A. (2019). Current and Future Variations of the Monsoons of the Americas in a Warming Climate. *Current Climate Change Reports, 5*(3), 125-144. journal article. https://doi.org/10.1007/s40641-019-00135-w

Phillips, T. J., Potter, G. L., Williamson, D. L., Cederwall, R. T., Boyle, J. S., Fiorino, M., et al. (2004). Evaluating Parameterizations in General Circulation Models: Climate Simulation Meets Weather Prediction. *Bulletin of the American Meteorological Society, 85*(12), 1903-1916. https://journals.ametsoc.org/view/journals/bams/85/12/bams-85-12-1903.xml

Qin, H. C., Pritchard, M. S., Kooperman, G. J., & Parishani, H. (2018). Global Effects of Superparameterization on Hydrothermal Land-Atmosphere Coupling on Multiple Timescales. *Journal of Advances in Modeling Earth Systems, 10*(2), 530-549. <Go to ISI>://WOS:000430297000016

Rasmussen, K. L., & Houze, R. A. (2016). Convective Initiation near the Andes in Subtropical South America. *Monthly Weather Review, 144*(6), 2351-2374. <Go to ISI>://WOS:000377449700005

Raymond, D. J., & Blyth, A. M. (1986). A Stochastic Mixing Model for Nonprecipitating Cumulus Clouds. *Journal of the Atmospheric Sciences, 43*(22), 2708-2718. <Go to ISI>://WOS:A1986F894400012

Raymond, D. J., & Blyth, A. M. (1992). Extension of the Stochastic Mixing Model to Cumulonimbus Clouds. *Journal of the Atmospheric Sciences, 49*(21), 1968-1983. <Go to ISI>://WOS:A1992JV90300002

Richter, J. H., & Rasch, P. J. (2008). Effects of convective momentum transport on the atmospheric circulation in the community atmosphere model, version 3. *Journal of Climate, 21*(7), 1487-1499. <Go to ISI>://WOS:000255004000003

Ruiz-Hernández, J.-C., Condom, T., Ribstein, P., Le Moine, N., Espinoza, J.-C., Junquas, C., et al. (2021). Spatial variability of diurnal to seasonal cycles of precipitation from a high-altitude equatorial Andean valley to the Amazon Basin. *Journal of Hydrology: Regional Studies, 38*, 100924. https://www.sciencedirect.com/science/article/pii/S2214581821001531
https://www.sciencedirect.com/science/article/pii/S2214581821001531?via%3Dihub

Sakaguchi, K., Leung, L. R., Burleyson, C. D., Xiao, H., & Wan, H. (2018). Role of Troposphere-Convection-Land Coupling in the Southwestern Amazon Precipitation Bias of the Community Earth System Model Version 1 (CESM1). *JOURNAL OF GEOPHYSICAL RESEARCH-ATMOSPHERES, 123*(16), 8374-8399. <Go to ISI>://WOS:000445331900002

Seiler, C., Hutjes, R. W. A., & Kabat, P. (2013). Likely Ranges of Climate Change in Bolivia. *Journal of Applied Meteorology and Climatology, 52*(6), 1303-1317. https://journals.ametsoc.org/doi/abs/10.1175/JAMC-D-12-0224.1

Snyder, P. K. (2010). The Influence of Tropical Deforestation on the Northern Hemisphere Climate by Atmospheric Teleconnections. *EARTH INTERACTIONS, 14*. <Go to ISI>://WOS:000279073900001

Sun, J., & Pritchard, M. S. (2016). Effects of explicit convection on global land-atmosphere coupling in the superparameterized CAM. *Journal of Advances in Modeling Earth Systems, 8*(3), 1248-1269. <Go to ISI>://WOS:000387793500012

Thome Sena, A. C., & Magnusdottir, G. (2020). Projected End-of-Century Changes in the South American Monsoon in the CESM Large Ensemble. *Journal of Climate, 33*(18), 7859-7874. https://journals.ametsoc.org/view/journals/clim/33/18/jcliD190645.xml
https://journals.ametsoc.org/downloadpdf/view/journals/clim/33/18/jcliD190645.pdf

An edited version of this paper was published by AGU. Published (2025) American Geophysical Union.
Qin, H., Pritchard, M., Terai, C. R., Bacmeister, J., Bogenschutz, P., & Kiladis, G. N. (2025). Remote influence of Andean convection on Amazonian rainfall and its mechanisms. Journal of Geophysical Research: Atmospheres, 130, e2025JD043465. https://doi.org/10.1029/2025JD043465

Tian, B., Manning, E., Roman, J., Thrastarson, H., Fetzer, E. J., & Monarrez, R. (2020). *AIRS Version 7 Level 3 Product User Guide*. Retrieved from https://docserver.gesdisc.eosdis.nasa.gov/public/project/AIRS/V7_L3_User_Guide.pdf

Tian, B. J., Fetzer, E. J., Kahn, B. H., Teixeira, J., Manning, E., & Hearty, T. (2013). Evaluating CMIP5 models using AIRS tropospheric air temperature and specific humidity climatology. *JOURNAL OF GEOPHYSICAL RESEARCH-ATMOSPHERES, 118*(1), 114-134. <Go to ISI>://WOS:000317834900009

Urrutia, R., & Vuille, M. (2009). Climate change projections for the tropical Andes using a regional climate model: Temperature and precipitation simulations for the end of the 21st century. *Journal of Geophysical Research: Atmospheres, 114*(D2). https://agupubs.onlinelibrary.wiley.com/doi/abs/10.1029/2008JD011021

Vizy, E. K., & Cook, K. H. (2007). Relationship between Amazon and high Andes rainfall. *JOURNAL OF GEOPHYSICAL RESEARCH-ATMOSPHERES, 112*(D7). <Go to ISI>://WOS:000245580500009

Werth, D., & Avissar, R. (2002). The local and global effects of Amazon deforestation. *JOURNAL OF GEOPHYSICAL RESEARCH-ATMOSPHERES, 107*(D20). <Go to ISI>://WOS:000180466200096

Xie, S., Wang, Y.-C., Lin, W., Ma, H.-Y., Tang, Q., Tang, S., et al. (2019). Improved Diurnal Cycle of Precipitation in E3SM With a Revised Convective Triggering Function. *Journal of Advances in Modeling Earth Systems, 11*(7), 2290-2310. https://agupubs.onlinelibrary.wiley.com/doi/abs/10.1029/2019MS001702

https://agupubs.onlinelibrary.wiley.com/doi/pdfdirect/10.1029/2019MS001702?download=true

Xie, S. C., Wang, Y. C., Lin, W. Y., Ma, H. Y., Tang, Q., Tang, S. Q., et al. (2019). Improved Diurnal Cycle of Precipitation in E3SM With a Revised Convective Triggering Function. *Journal of Advances in Modeling Earth Systems, 11*(7), 2290-2310. <Go to ISI>://WOS:000480282800019

https://agupubs.onlinelibrary.wiley.com/doi/full/10.1029/2019MS001702

Yazdandoost, F., Moradian, S., Izadi, A., & Aghakouchak, A. (2021). Evaluation of CMIP6 precipitation simulations across different climatic zones: Uncertainty and model intercomparison. *Atmospheric Research, 250*, 105369. https://www.sciencedirect.com/science/article/pii/S0169809520313065

Yin, L., Fu, R., Shevliakova, E., & Dickinson, R. E. (2012). How well can CMIP5 simulate precipitation and its controlling processes over tropical South America? *Climate Dynamics, 41*(11-12), 3127-3143. https://doi.org/10.1007/s00382-012-1582-y

https://link.springer.com/content/pdf/10.1007%2Fs00382-012-1582-y.pdf

Zhang, G. J., & Mcfarlane, N. A. (1995). Sensitivity of Climate Simulations to the Parameterization of Cumulus Convection in the Canadian Climate Center General-Circulation Model. *Atmosphere-Ocean, 33*(3), 407-446. <Go to ISI>://WOS:A1995RW15200002

Zhang, K., Fu, R., Shaikh, M. J., Ghan, S., Wang, M., Leung, L. R., et al. (2017). Influence of Superparameterization and a Higher-Order Turbulence Closure on Rainfall Bias Over Amazonia in Community Atmosphere Model Version 5. *Journal of Geophysical Research: Atmospheres, 122*(18), 9879-9902. https://agupubs.onlinelibrary.wiley.com/doi/abs/10.1002/2017JD026576

https://agupubs.onlinelibrary.wiley.com/doi/pdf/10.1002/2017JD026576

Supporting Information References

Bi, D., Dix, M., Marsland, S., O'Farrell, S., Sullivan, A., Bodman, R., et al. (2020). Configuration and spin-up of ACCESS-CM2, the new generation Australian Community Climate and Earth System Simulator Coupled Model. *Journal of Southern Hemisphere Earth Systems Science, 70*(1), 225-251. https://www.publish.csiro.au/paper/ES19040

Boucher, O., Servonnat, J., Albright, A. L., Aumont, O., Balkanski, Y., Bastrikov, V., et al. (2020). Presentation and Evaluation of the IPSL-CM6A-LR Climate Model. *Journal of Advances in Modeling Earth Systems, 12*(7), e2019MS002010. https://agupubs.onlinelibrary.wiley.com/doi/abs/10.1029/2019MS002010

Cao, J., Wang, B., Yang, Y. M., Ma, L., Li, J., Sun, B., et al. (2018). The NUIST Earth System Model (NESM) version 3: description and preliminary evaluation. *Geosci. Model Dev., 11*(7), 2975-2993. https://gmd.copernicus.org/articles/11/2975/2018/

CHEN, H.-M., LI, J., SU, J.-Z., HUA, L.-J., RONG, X.-Y., XIN, Y.-F., & ZHANG, Z.-Q. (2019). Introduction of CAMS-CSM model and its participation in CMIP6. *Advances in Climate Change Research, 15*(5), 540-544. http://www.climatechange.cn/EN/10.12006/j.issn.1673-1719.2019.186

http://www.climatechange.cn/CN/10.12006/j.issn.1673-1719.2019.186

An edited version of this paper was published by AGU. Published (2025) American Geophysical Union.
Qin, H., Pritchard, M., Terai, C. R., Bacmeister, J., Bogenschutz, P., & Kiladis, G. N. (2025). Remote influence of Andean convection on Amazonian rainfall and its mechanisms. Journal of Geophysical Research: Atmospheres, 130, e2025JD043465. https://doi.org/10.1029/2025JD043465

Cherchi, A., Fogli, P. G., Lovato, T., Peano, D., Iovino, D., Gualdi, S., et al. (2019). Global Mean Climate and Main Patterns of Variability in the CMCC-CM2 Coupled Model. *Journal of Advances in Modeling Earth Systems, 11*(1), 185-209. https://agupubs.onlinelibrary.wiley.com/doi/abs/10.1029/2018MS001369

Danabasoglu, G., Lamarque, J.-F., Bacmeister, J., Bailey, D. A., DuVivier, A. K., Edwards, J., et al. (2020). The Community Earth System Model Version 2 (CESM2). *Journal of Advances in Modeling Earth Systems, 12*(2), e2019MS001916. https://agupubs.onlinelibrary.wiley.com/doi/abs/10.1029/2019MS001916

Döscher, R., Acosta, M., Alessandri, A., Anthoni, P., Arsouze, T., Bergman, T., et al. (2022). The EC-Earth3 Earth system model for the Coupled Model Intercomparison Project 6. *Geosci. Model Dev., 15*(7), 2973-3020. https://gmd.copernicus.org/articles/15/2973/2022/

Dunne, J. P., Horowitz, L. W., Adcroft, A. J., Ginoux, P., Held, I. M., John, J. G., et al. (2020). The GFDL Earth System Model Version 4.1 (GFDL-ESM 4.1): Overall Coupled Model Description and Simulation Characteristics. *Journal of Advances in Modeling Earth Systems, 12*(11), e2019MS002015. https://agupubs.onlinelibrary.wiley.com/doi/abs/10.1029/2019MS002015

Gettelman, A., Mills, M. J., Kinnison, D. E., Garcia, R. R., Smith, A. K., Marsh, D. R., et al. (2019). The Whole Atmosphere Community Climate Model Version 6 (WACCM6). *Journal of Geophysical Research: Atmospheres, 124*(23), 12380-12403. https://agupubs.onlinelibrary.wiley.com/doi/abs/10.1029/2019JD030943

Golaz, J. C., Caldwell, P. M., Van Roekel, L. P., Petersen, M. R., Tang, Q., Wolfe, J. D., et al. (2019). The DOE E3SM Coupled Model Version 1: Overview and Evaluation at Standard Resolution. *Journal of Advances in Modeling Earth Systems, 11*(7), 2089-2129. <Go to ISI>://WOS:000480282800012
https://agupubs.onlinelibrary.wiley.com/doi/full/10.1029/2018MS001603

Hajima, T., Watanabe, M., Yamamoto, A., Tatebe, H., Noguchi, M. A., Abe, M., et al. (2020). Development of the MIROC-ES2L Earth system model and the evaluation of biogeochemical processes and feedbacks. *Geosci. Model Dev., 13*(5), 2197-2244. https://gmd.copernicus.org/articles/13/2197/2020/

He, B., Yu, Y., Bao, Q., Lin, P., Liu, H., Li, J., et al. (2020). CAS FGOALS-f3-L model dataset descriptions for CMIP6 DECK experiments. *Atmospheric and Oceanic Science Letters, 13*(6), 582-588. https://doi.org/10.1080/16742834.2020.1778419

Hill, S. A., Ming, Y., Held, I. M., & Zhao, M. (2017). A Moist Static Energy Budget–Based Analysis of the Sahel Rainfall Response to Uniform Oceanic Warming. *Journal of Climate, 30*(15), 5637-5660. https://journals.ametsoc.org/view/journals/clim/30/15/jcli-d-16-0785.1.xml

Inoue, K., & Back, L. (2015). Column-Integrated Moist Static Energy Budget Analysis on Various Time Scales during TOGA COARE. *Journal of the Atmospheric Sciences, 72*(5), 1856-1871. <Go to ISI>://WOS:000353840100010

Kelley, M., Schmidt, G. A., Nazarenko, L. S., Bauer, S. E., Ruedy, R., Russell, G. L., et al. (2020). GISS-E2.1: Configurations and Climatology. *Journal of Advances in Modeling Earth Systems, 12*(8), e2019MS002025. https://doi.org/10.1029/2019MS002025

Krishnan, R., Swapna, P., Vellore, R., Narayanasetti, S., Prajeesh, A. G., Choudhury, A. D., et al. (2019). The IITM Earth System Model (ESM): Development and Future Roadmap. In D. A. Randall, J. Srinivasan, R. S. Nanjundiah, & P. Mukhopadhyay (Eds.), *Current Trends in the Representation of Physical Processes in Weather and Climate Models* (pp. 183-195). Singapore: Springer Singapore.

Lee, J., Kim, J., Sun, M.-A., Kim, B.-H., Moon, H., Sung, H. M., et al. (2020). Evaluation of the Korea Meteorological Administration Advanced Community Earth-System model (K-ACE). *Asia-Pacific Journal of Atmospheric Sciences, 56*(3), 381-395. https://doi.org/10.1007/s13143-019-00144-7

Lee, W. L., Wang, Y. C., Shiu, C. J., Tsai, I., Tu, C. Y., Lan, Y. Y., et al. (2020). Taiwan Earth System Model Version 1: description and evaluation of mean state. *Geosci. Model Dev., 13*(9), 3887-3904. https://gmd.copernicus.org/articles/13/3887/2020/

Lin, Y., Huang, X., Liang, Y., Qin, Y., Xu, S., Huang, W., et al. (2020). Community Integrated Earth System Model (CIESM): Description and Evaluation. *Journal of Advances in Modeling Earth Systems, 12*(8), e2019MS002036. https://agupubs.onlinelibrary.wiley.com/doi/abs/10.1029/2019MS002036

Mauritsen, T., Bader, J., Becker, T., Behrens, J., Bittner, M., Brokopf, R., et al. (2019). Developments in the MPI-M Earth System Model version 1.2 (MPI-ESM1.2) and Its Response to Increasing CO2. *Journal of Advances in Modeling Earth Systems, 11*(4), 998-1038. https://agupubs.onlinelibrary.wiley.com/doi/abs/10.1029/2018MS001400

Müller, W. A., Jungclaus, J. H., Mauritsen, T., Baehr, J., Bittner, M., Budich, R., et al. (2018). A Higher-resolution Version of the Max Planck Institute Earth System Model (MPI-ESM1.2-HR). *Journal of Advances in*

Modeling Earth Systems, 10(7), 1383-1413. https://agupubs.onlinelibrary.wiley.com/doi/abs/10.1029/2017MS001217

Park, S., Shin, J., Kim, S., Oh, E., & Kim, Y. (2019). Global Climate Simulated by the Seoul National University Atmosphere Model Version 0 with a Unified Convection Scheme (SAM0-UNICON). *Journal of Climate, 32*(10), 2917-2949. https://journals.ametsoc.org/view/journals/clim/32/10/jcli-d-18-0796.1.xml

Raymond, D. J., Sessions, S. L., Sobel, A. H., & Fuchs, Z. (2009). The Mechanics of Gross Moist Stability. *Journal of Advances in Modeling Earth Systems, 1*(3), n/a-n/a. <Go to ISI>://WOS:000208299400009

Séférian, R., Nabat, P., Michou, M., Saint-Martin, D., Voldoire, A., Colin, J., et al. (2019). Evaluation of CNRM Earth System Model, CNRM-ESM2-1: Role of Earth System Processes in Present-Day and Future Climate. *Journal of Advances in Modeling Earth Systems, 11*(12), 4182-4227. https://agupubs.onlinelibrary.wiley.com/doi/abs/10.1029/2019MS001791

Seland, Ø., Bentsen, M., Olivié, D., Toniazzo, T., Gjermundsen, A., Graff, L. S., et al. (2020). Overview of the Norwegian Earth System Model (NorESM2) and key climate response of CMIP6 DECK, historical, and scenario simulations. *Geosci. Model Dev., 13*(12), 6165-6200. https://gmd.copernicus.org/articles/13/6165/2020/

Sellar, A. A., Jones, C. G., Mulcahy, J. P., Tang, Y., Yool, A., Wiltshire, A., et al. (2019). UKESM1: Description and Evaluation of the U.K. Earth System Model. *Journal of Advances in Modeling Earth Systems, 11*(12), 4513-4558. https://agupubs.onlinelibrary.wiley.com/doi/abs/10.1029/2019MS001739

Swart, N. C., Cole, J. N. S., Kharin, V. V., Lazare, M., Scinocca, J. F., Gillett, N. P., et al. (2019). The Canadian Earth System Model version 5 (CanESM5.0.3). *Geosci. Model Dev., 12*(11), 4823-4873. https://gmd.copernicus.org/articles/12/4823/2019/

Tatebe, H., Ogura, T., Nitta, T., Komuro, Y., Ogochi, K., Takemura, T., et al. (2019). Description and basic evaluation of simulated mean state, internal variability, and climate sensitivity in MIROC6. *Geosci. Model Dev., 12*(7), 2727-2765. https://gmd.copernicus.org/articles/12/2727/2019/

Tegen, I., Neubauer, D., Ferrachat, S., Siegenthaler-Le Drian, C., Bey, I., Schutgens, N., et al. (2019). The global aerosol–climate model ECHAM6.3–HAM2.3 – Part 1: Aerosol evaluation. *Geosci. Model Dev., 12*(4), 1643-1677. https://gmd.copernicus.org/articles/12/1643/2019/

Voldoire, A., Saint-Martin, D., Sénési, S., Decharme, B., Alias, A., Chevallier, M., et al. (2019). Evaluation of CMIP6 DECK Experiments With CNRM-CM6-1. *Journal of Advances in Modeling Earth Systems, 11*(7), 2177-2213. https://agupubs.onlinelibrary.wiley.com/doi/abs/10.1029/2019MS001683

Volodin, E. M., Diansky, N. A., & Gusev, A. V. (2013). Simulation and prediction of climate changes in the 19th to 21st centuries with the Institute of Numerical Mathematics, Russian Academy of Sciences, model of the Earth's climate system. *Izvestiya, Atmospheric and Oceanic Physics, 49*(4), 347-366. https://doi.org/10.1134/S0001433813040105

Volodin, E. M., Mortikov, E. V., Kostrykin, S. V., Galin, V. Y., Lykosov, V. N., Gritsun, A. S., et al. (2017). Simulation of modern climate with the new version of the INM RAS climate model. *Izvestiya, Atmospheric and Oceanic Physics, 53*(2), 142-155. https://doi.org/10.1134/S0001433817020128

Williams, K. D., Copsey, D., Blockley, E. W., Bodas-Salcedo, A., Calvert, D., Comer, R., et al. (2018). The Met Office Global Coupled Model 3.0 and 3.1 (GC3.0 and GC3.1) Configurations. *Journal of Advances in Modeling Earth Systems, 10*(2), 357-380. https://agupubs.onlinelibrary.wiley.com/doi/abs/10.1002/2017MS001115

Wu, T., Lu, Y., Fang, Y., Xin, X., Li, L., Li, W., et al. (2019). The Beijing Climate Center Climate System Model (BCC-CSM): the main progress from CMIP5 to CMIP6. *Geosci. Model Dev., 12*(4), 1573-1600. https://gmd.copernicus.org/articles/12/1573/2019/

Wu, T., Zhang, F., Zhang, J., Jie, W., Zhang, Y., Wu, F., et al. (2020). Beijing Climate Center Earth System Model version 1 (BCC-ESM1): model description and evaluation of aerosol simulations. *Geosci. Model Dev., 13*(3), 977-1005. https://gmd.copernicus.org/articles/13/977/2020/

Yukimoto, S., Kawai, H., Koshiro, T., Oshima, N., Yoshida, K., Urakawa, S., et al. (2019). The Meteorological Research Institute Earth System Model Version 2.0, MRI-ESM2.0: Description and Basic Evaluation of the Physical Component. *Journal of the Meteorological Society of Japan. Ser. II, 97*(5), 931-965.

Ziehn, T., Chamberlain, M. A., Law, R. M., Lenton, A., Bodman, R. W., Dix, M., et al. (2020). The Australian Earth System Model: ACCESS-ESM1.5. *Journal of Southern Hemisphere Earth Systems Science, 70*(1), 193-214. https://www.publish.csiro.au/paper/ES19035

An edited version of this paper was published by AGU. Published (2025) American Geophysical Union.
Qin, H., Pritchard, M., Terai, C. R., Bacmeister, J., Bogenschutz, P., & Kiladis, G. N. (2025). Remote influence of Andean convection on Amazonian rainfall and its mechanisms. Journal of Geophysical Research: Atmospheres, 130, e2025JD043465. https://doi.org/10.1029/2025JD043465

Figure Captions

Figure 1. (a) Comparing to Global Precipitation Climatology Project (GPCP) v2.3 (R. F. Adler et al., 2003; G. J. Huffman et al., 2009), 1989-2008 annual mean rainfall biases of the multi-model-mean of 39 models in the AMIP-type simulations of CMIP6 archive (see Table S1). Units: mm/day. (b) Similar to (a) but for Dec-Jan-Feb (DJF) months only. (c) Relative to GPCP v2.3, 1989-2008 DJF mean rainfall bias in the CESM v1.1 control simulation. The Amazon box in red (64°W-50°W, 14°S-0°) represents an area with large dry bias of precipitation. (d) Control simulation 1989-2008 DJF mean rainfall. Units: mm/day.

Figure 2. (a) Interference based on topography height (h = surface geopotential PHIS divided by gravitational acceleration 9.8 m/sec^2) within the Andean region (50 °S-10°N, 90°W-60°W). At the time-step level, temperature tendencies from convective processes are untouched if $h < 500m$ (purple color), linearly damped if $500m \leq h < 600m$ (beige color), and fully muted if $h \geq 600m$ (pink color). Units: meter. (b) The linear ramp function used in the interference based on topography height.

Figure 3. Diurnal cycle (in local time phase) and amplitude (in mm/day) of the first harmonic of total precipitation in CTR during DJF from 1998-2008 (first row) and TRMM 3B42 during DJF from 1998-2008 (second row). CTR has hourly data and TRMM 3B42 has 3-hourly data. The earliest data availability from TRMM is 1998. Diurnal peak time is represented by the color hue and amplitude is represented by the color saturation.

Figure 4. (a) Hovmöller diagram showing the composite diurnal cycle of equatorial rainfall (shading) in the CTR ensemble (180 members), averaged between 5°S-5°N, with contours showing the vertically integrated (1000-100hPa) Andean forcing in the CTR group which is denied in the TOPO group. Units: precipitation in mm/day, forcing in W/m^2. (b) Composite height-longitude snapshot at 10°S latitude, showing Andean forcing in the CTR group at the 18th hour after branching off (13:00 local time at 75°W). Units: K/day. (c) As in (b) but showing the horizontal structure of the vertically integrated (1000-100hPa) Andean forcing in the CTR group. Units: W/m^2.

Figure 5. (a) Precipitation responses to Andean forcing (CTR minus TOPO) at the 13th hour after branching off. Stippling shows 0.05 significance level in the student-t test. The Amazon area is defined within the red box (64°W-50°W, 14°S-0°N), same as shown in Figure 1(c). Units: mm/day. (b) Time series of precipitation averaged over the Amazon box in the CTR group. The orange curve indicates TRMM reference calculated from 1998-2008 DJF. Units: mm/day. (c) Time series of the differences in precipitation averaged over the Amazon box between CTR and TOPO group. Units: mm/day. In (b) and (c), bars indicate 95% confidence interval. Grey shading indicates local nighttime hours (18:00-06:00 local time at 60°W). In (c), difference of precipitation between CTR and TOPO during 120-240 hours resambles patterns seen in day 4-5 and is indistinguishable from zero and thus not shown. Time series of each individual member is shown in Figure S2.

An edited version of this paper was published by AGU. Published (2025) American Geophysical Union.
Qin, H., Pritchard, M., Terai, C. R., Bacmeister, J., Bogenschutz, P., & Kiladis, G. N. (2025). Remote influence of Andean convection on Amazonian rainfall and its mechanisms. Journal of Geophysical Research: Atmospheres, 130, e2025JD043465. https://doi.org/10.1029/2025JD043465

Figure 6. Differences of time series in a variety of diagnostics between CTR and TOPO group averaged over the Amazon box shown in Figure 5(a). (a) Moist Static Energy (blue), Latent Static Energy $\boldsymbol{L_v q}$ (yellow), and Dry Static Energy $\boldsymbol{C_p T + gz}$ (green) averaged over the lowest five model layers. Units: kJ/kg. (b) Surface sensible heat flux (blue), surface latent heat flux (yellow), vertically integrated solar heating rate (green), vertically integrated longwave heating rate (red), the sum of the four terms (purple). Units: watts/m^2. (c) The local rate of change in vertically integrated specific humidity (blue) calculated based on equation (2.1), vertically integrated total physics tendency of specific humidity PTEQ (yellow), vertically integrated total advection of specific humidity (green) inferred based on equation (2.2). Units: g/kg/hr. (d) Convective Available Potential Energy (CAPE). Units: J/kg. (e) Decomposition of the total advection of specific humidity based on equation (2.5). Vertical integral of the horizontal advection of specific humidity $-(\boldsymbol{u}\frac{\partial \boldsymbol{q}}{\partial \boldsymbol{x}} + \boldsymbol{v}\frac{\partial \boldsymbol{q}}{\partial \boldsymbol{y}})$ (blue), vertical integral of the divergence term $-\boldsymbol{q}(\frac{\partial \boldsymbol{u}}{\partial \boldsymbol{x}} + \frac{\partial \boldsymbol{v}}{\partial \boldsymbol{y}})$ (yellow), vertical integral of the vertical advective term $-\boldsymbol{\omega}\frac{\partial \boldsymbol{q}}{\partial \boldsymbol{p}}$ (green), vertical integral of the vertical gradient term $-\boldsymbol{q}\frac{\partial \boldsymbol{\omega}}{\partial \boldsymbol{p}}$ (red). Units: g/kg/hr. (f) The sum of the previous four terms in panel c (blue), and vertical integral of the total advection of specific humidity inferred based on equation (2.2) (yellow). Units: g/kg/hr. (g) Differences of the vertically integrated vertical advection of specific humidity between CTR and TOPO group $\langle -\boldsymbol{\omega}\frac{\partial \boldsymbol{q}}{\partial \boldsymbol{p}}\rangle_{\boldsymbol{CTR-TOPO}}$ (blue), and its decomposition into three terms based on equation (2.7), $-\langle \boldsymbol{\omega}_{\boldsymbol{TOPO}}\left[\frac{\partial \boldsymbol{q}}{\partial \boldsymbol{p}}\right]_{\boldsymbol{CTR-TOPO}}\rangle$ in yellow, $-\langle \boldsymbol{\omega}_{\boldsymbol{CTR-TOPO}}\left[\frac{\partial \boldsymbol{q}}{\partial \boldsymbol{p}}\right]_{\boldsymbol{TOPO}}\rangle$ in green, $-\langle \boldsymbol{\omega}_{\boldsymbol{CTR-TOPO}}\left[\frac{\partial \boldsymbol{q}}{\partial \boldsymbol{p}}\right]_{\boldsymbol{CTR-TOPO}}\rangle$ in red. Units: g/kg/hr. Note that the fact that the sum of three individual components does not seem to equal to the original term $\langle -\boldsymbol{\omega}\frac{\partial \boldsymbol{q}}{\partial \boldsymbol{p}}\rangle_{\boldsymbol{CTR-TOPO}}$ (blue). This is likely due to errors introduced in gradient calculations which would be accumulated in the summation. (h) precipitation response over the Amazon. Unit: mm/day.

Figure 7. Time series of vertical profiles of cloud fraction averaged over the Amazon (same as in Figure 5) in the CTR group (left) and in the CTR-minus-TOPO group (right). Units: unitless.

Figure 8. Transect at 10°S latitude. (a-d) Differences between CTR and TOPO group of temperature (shading), zonal, and vertical velocity (arrows), where vertical velocity is magnified 100 times for visibility. Units: temperature in, wind in m/sec. (e-h) Differences between CTR and TOPO group of specific humidity. Units: g/kg. (a)(e) show the 4th hour after branching off (23:00 local time at 75°W). (b)(f) show the 7th hour after branching off (02:00 local time at 75°W). (c)(g) show the 10th hour after branching off (05:00 local time at 75°W). (d)(h) show the 13th hour after branching off (08:00 local time at 75°W). Shading around 75°W represents Andean topography.

Figure 9. Hovmoller diagram for the first 96 hours after branching off, averaged over latitude of 5°N-5°S. Shading represents precipitation difference between CTR and TOPO (units: mm/day). Contours represent (a) 850hPa zonal wind difference between CTR and TOPO (units: m/sec); (b) 850hPa geopotential height difference between CTR and TOPO (units: m). Both shading and contours are only retained with a 0.1 significance level of student-t test. Note between the 16-

An edited version of this paper was published by AGU. Published (2025) American Geophysical Union.
Qin, H., Pritchard, M., Terai, C. R., Bacmeister, J., Bogenschutz, P., & Kiladis, G. N. (2025). Remote influence of Andean convection on Amazonian rainfall and its mechanisms. Journal of Geophysical Research: Atmospheres, 130, e2025JD043465. https://doi.org/10.1029/2025JD043465

995 28th hours, the eastward propagation speed of 850hPa geopotential height is about 50
996 meter/sec, within the range of phase speed of dry Kelvin waves between 30-60 meter/sec.
997
998 Figure 10. Snapshots of 850hPa wind vectors in the TOPO group (first row), and differences
999 between the CTR group and the TOPO group (second row). Unit: meter/sec. Differences are
1000 retained at 0.1 significance level of student-t test.
1001

An edited version of this paper was published by AGU. Published (2025) American Geophysical Union.
Qin, H., Pritchard, M., Terai, C. R., Bacmeister, J., Bogenschutz, P., & Kiladis, G. N. (2025). Remote influence of Andean convection on Amazonian rainfall and its mechanisms. Journal of Geophysical Research: Atmospheres, 130, e2025JD043465. https://doi.org/10.1029/2025JD043465

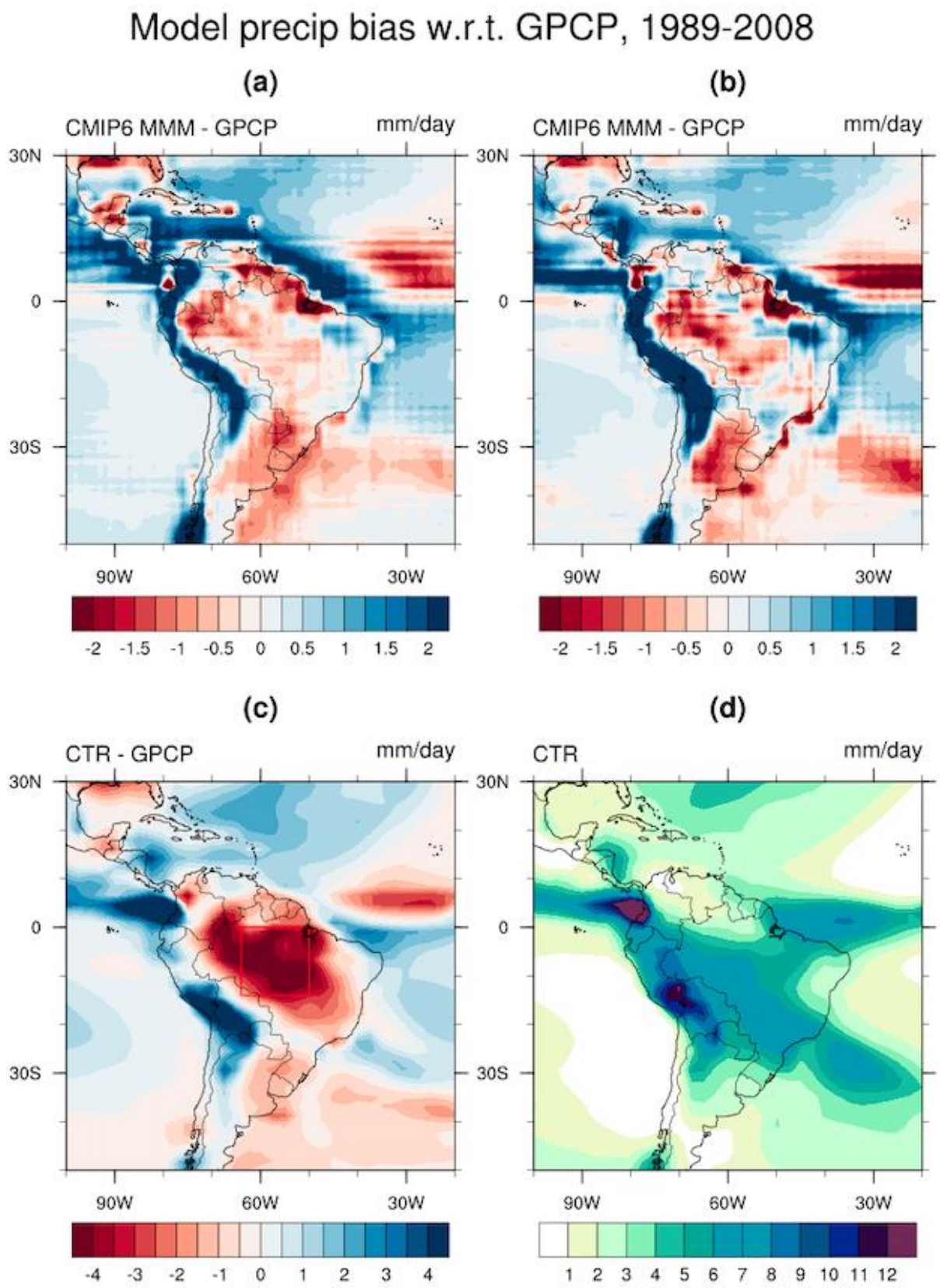

1002

An edited version of this paper was published by AGU. Published (2025) American Geophysical Union.
Qin, H., Pritchard, M., Terai, C. R., Bacmeister, J., Bogenschutz, P., & Kiladis, G. N. (2025). Remote influence of Andean convection on Amazonian rainfall and its mechanisms. Journal of Geophysical Research: Atmospheres, 130, e2025JD043465. https://doi.org/10.1029/2025JD043465

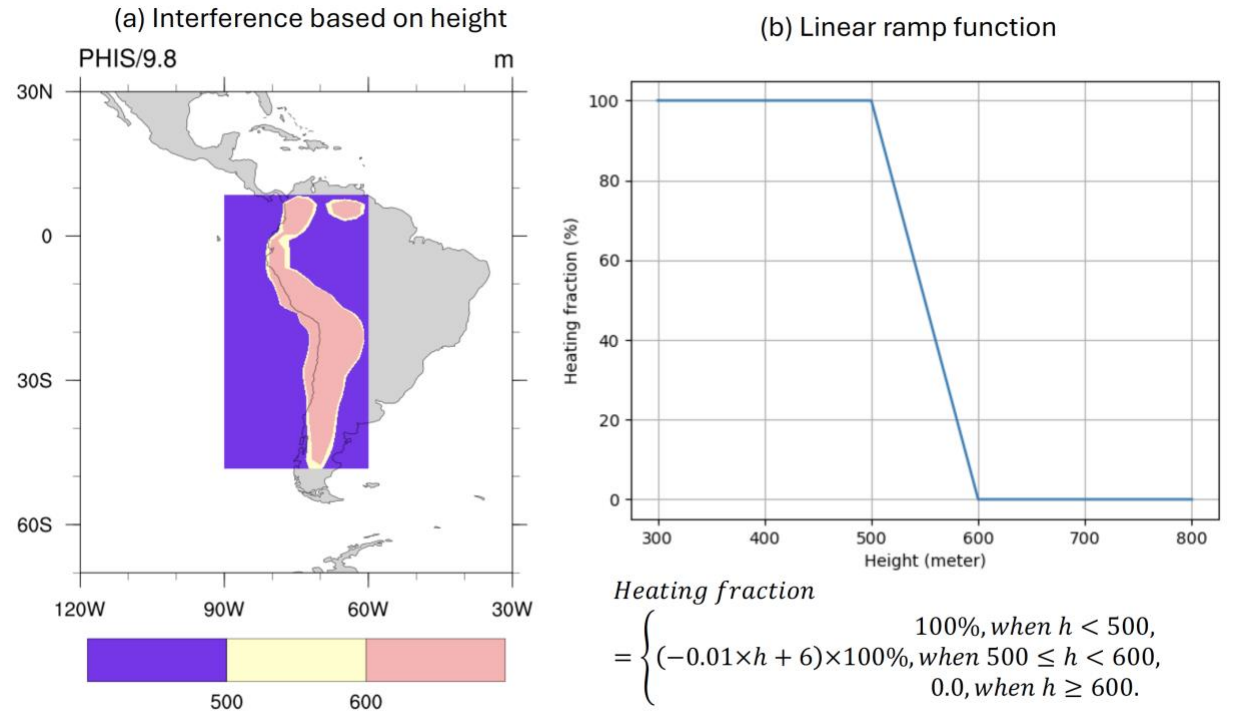

$$Heating\ fraction = \begin{cases} 100\%, when\ h < 500, \\ (-0.01 \times h + 6) \times 100\%, when\ 500 \le h < 600, \\ 0.0, when\ h \ge 600. \end{cases}$$

1003

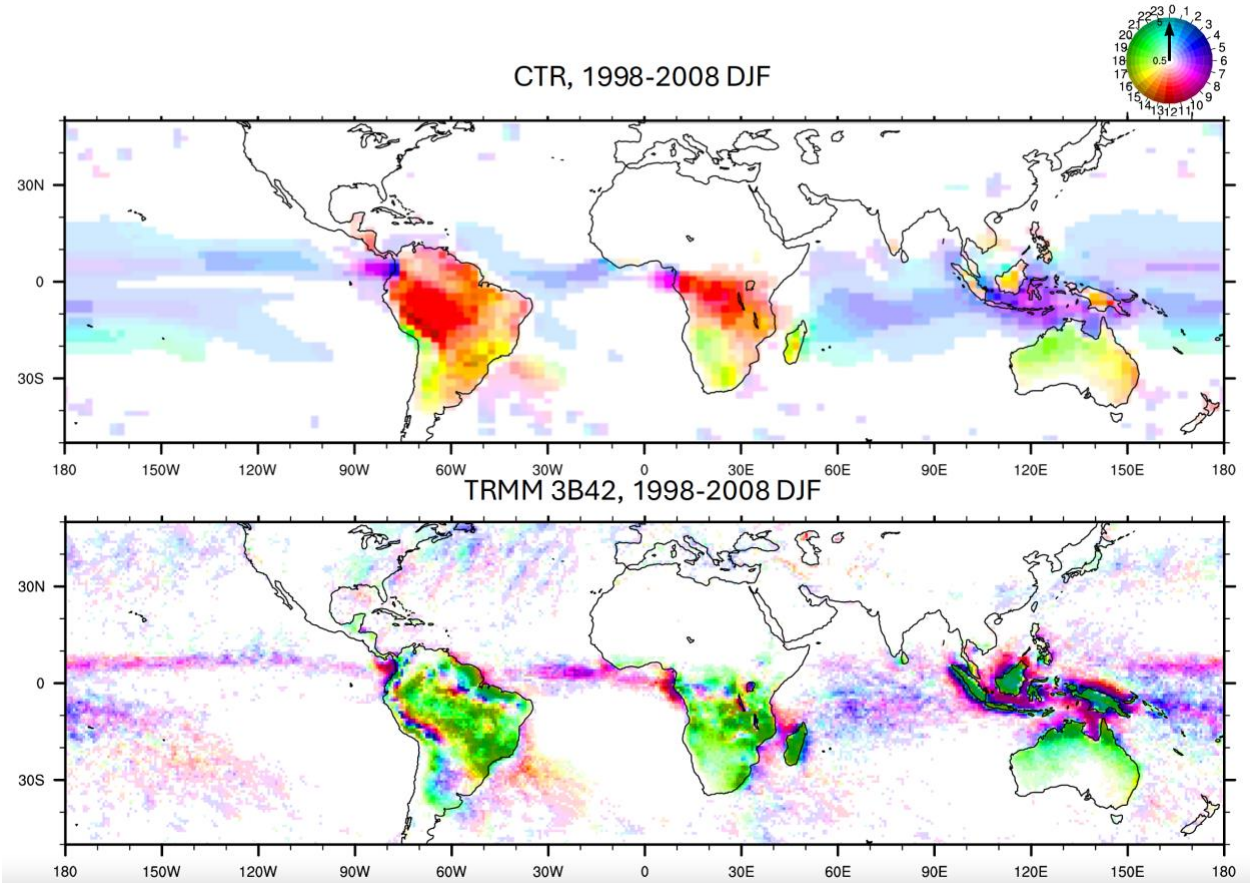

1004

An edited version of this paper was published by AGU. Published (2025) American Geophysical Union.
Qin, H., Pritchard, M., Terai, C. R., Bacmeister, J., Bogenschutz, P., & Kiladis, G. N. (2025). Remote influence of Andean convection on Amazonian rainfall and its mechanisms. Journal of Geophysical Research: Atmospheres, 130, e2025JD043465. https://doi.org/10.1029/2025JD043465

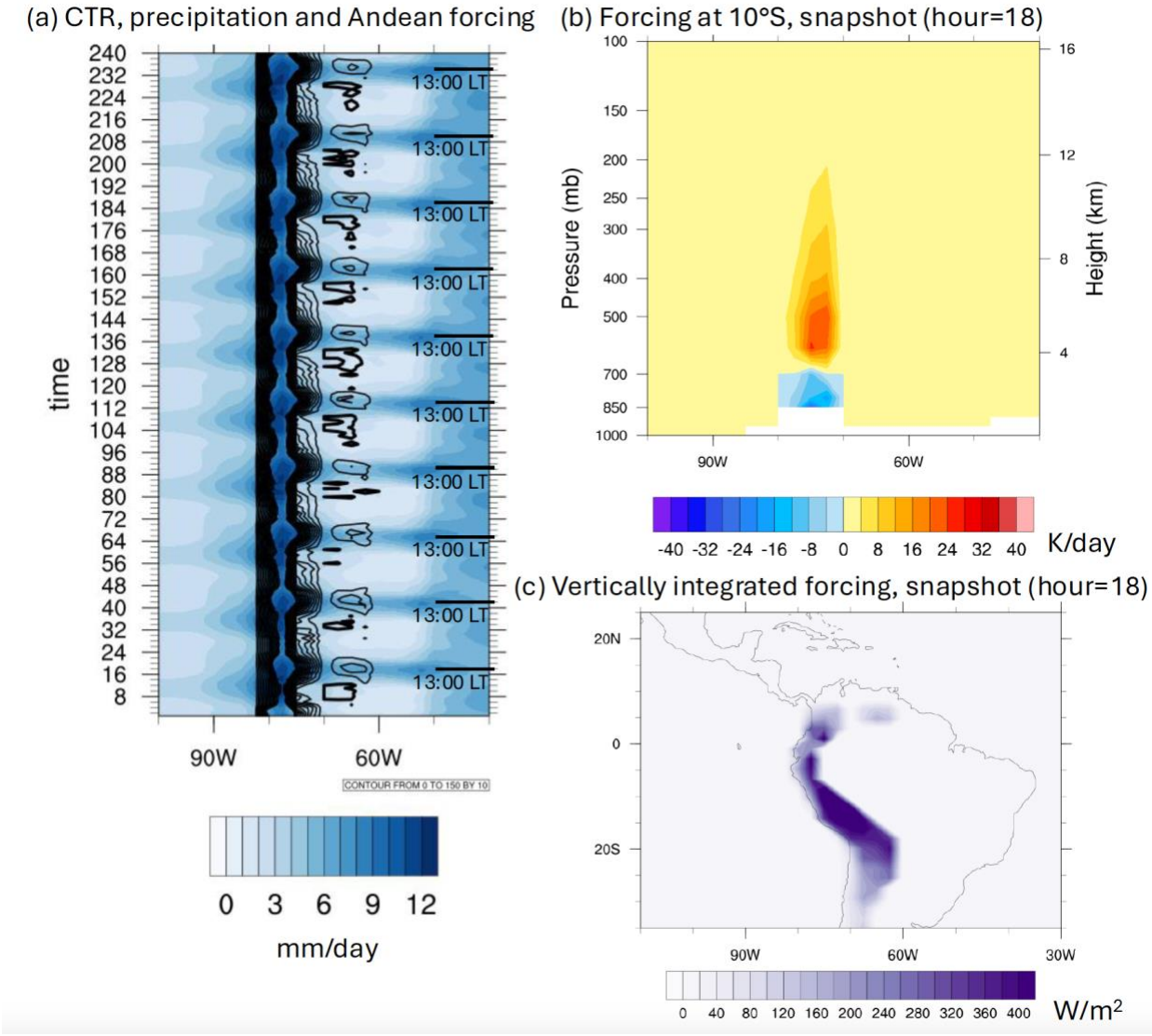

1005

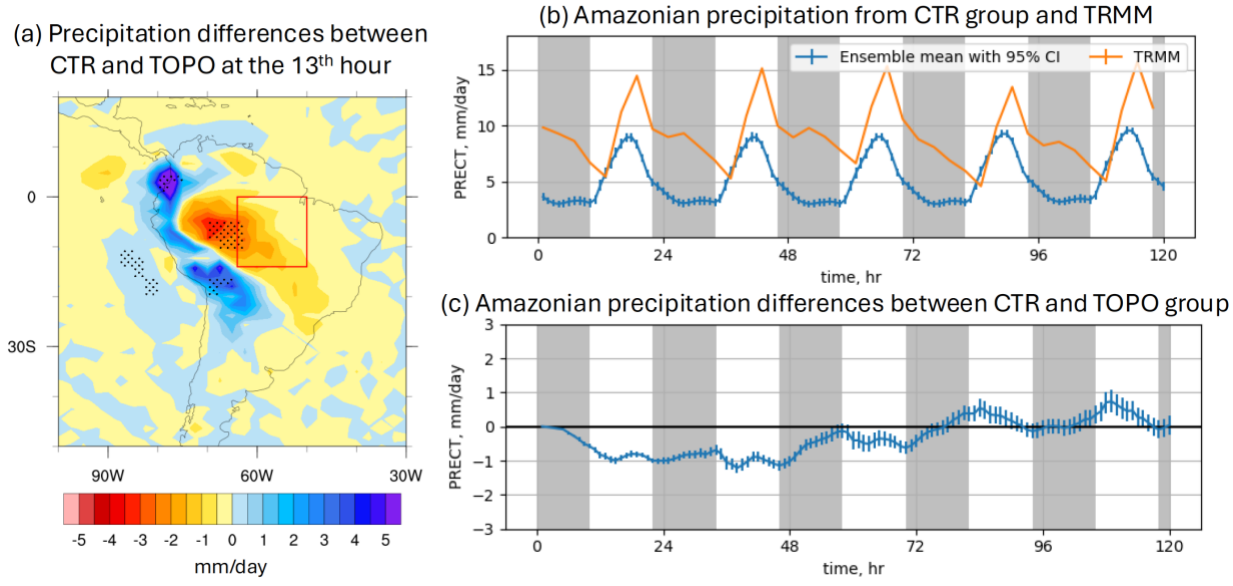

1006

An edited version of this paper was published by AGU. Published (2025) American Geophysical Union.
Qin, H., Pritchard, M., Terai, C. R., Bacmeister, J., Bogenschutz, P., & Kiladis, G. N. (2025). Remote influence of Andean convection on Amazonian rainfall and its mechanisms. Journal of Geophysical Research: Atmospheres, 130, e2025JD043465. https://doi.org/10.1029/2025JD043465

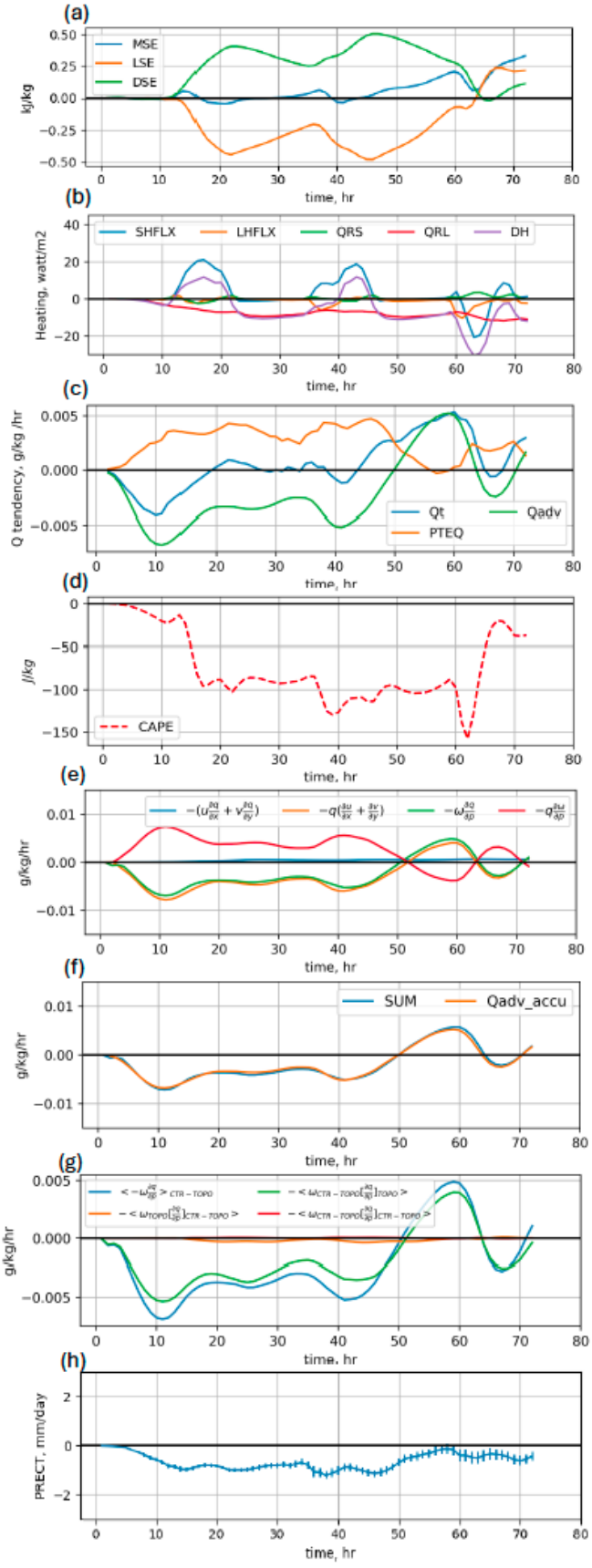

1007

An edited version of this paper was published by AGU. Published (2025) American Geophysical Union.
Qin, H., Pritchard, M., Terai, C. R., Bacmeister, J., Bogenschutz, P., & Kiladis, G. N. (2025). Remote influence of Andean convection on Amazonian rainfall and its mechanisms. Journal of Geophysical Research: Atmospheres, 130, e2025JD043465. https://doi.org/10.1029/2025JD043465

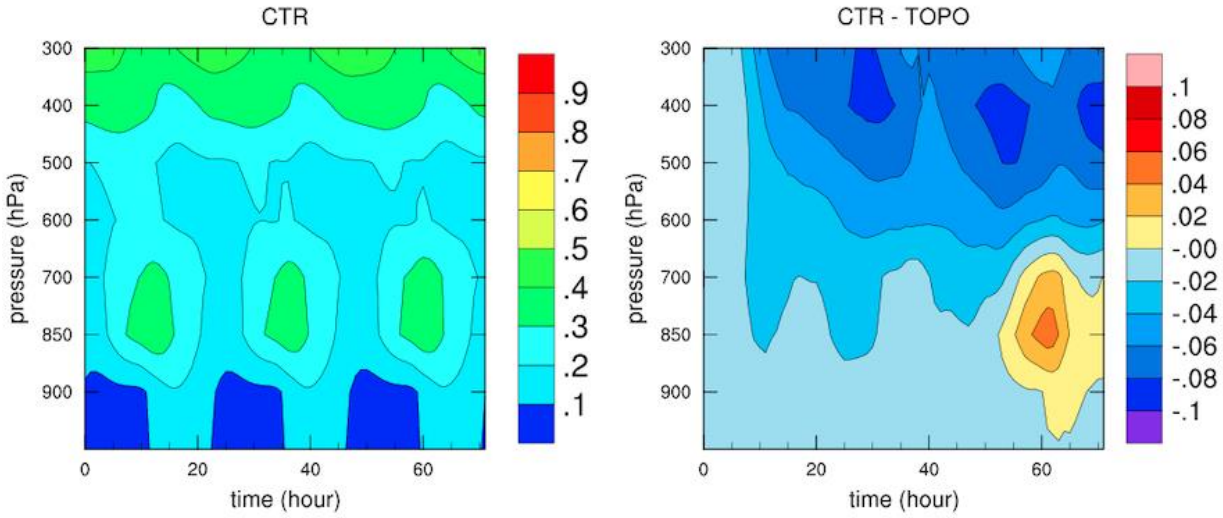

1008

An edited version of this paper was published by AGU. Published (2025) American Geophysical Union.
Qin, H., Pritchard, M., Terai, C. R., Bacmeister, J., Bogenschutz, P., & Kiladis, G. N. (2025). Remote influence of Andean convection on Amazonian rainfall and its mechanisms. Journal of Geophysical Research: Atmospheres, 130, e2025JD043465. https://doi.org/10.1029/2025JD043465

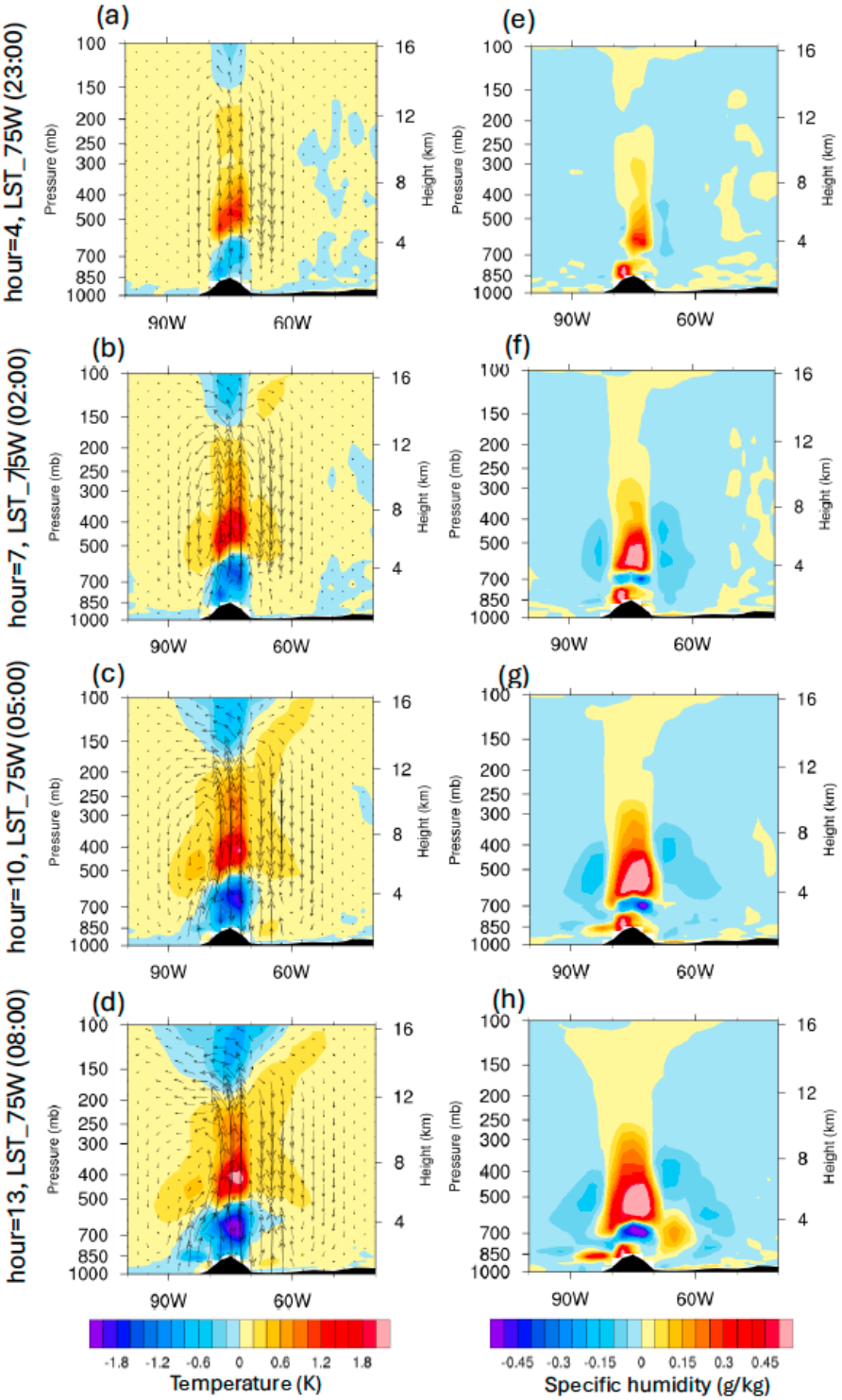

1009

An edited version of this paper was published by AGU. Published (2025) American Geophysical Union.
Qin, H., Pritchard, M., Terai, C. R., Bacmeister, J., Bogenschutz, P., & Kiladis, G. N. (2025). Remote influence of Andean convection on Amazonian rainfall and its mechanisms. Journal of Geophysical Research: Atmospheres, 130, e2025JD043465. https://doi.org/10.1029/2025JD043465

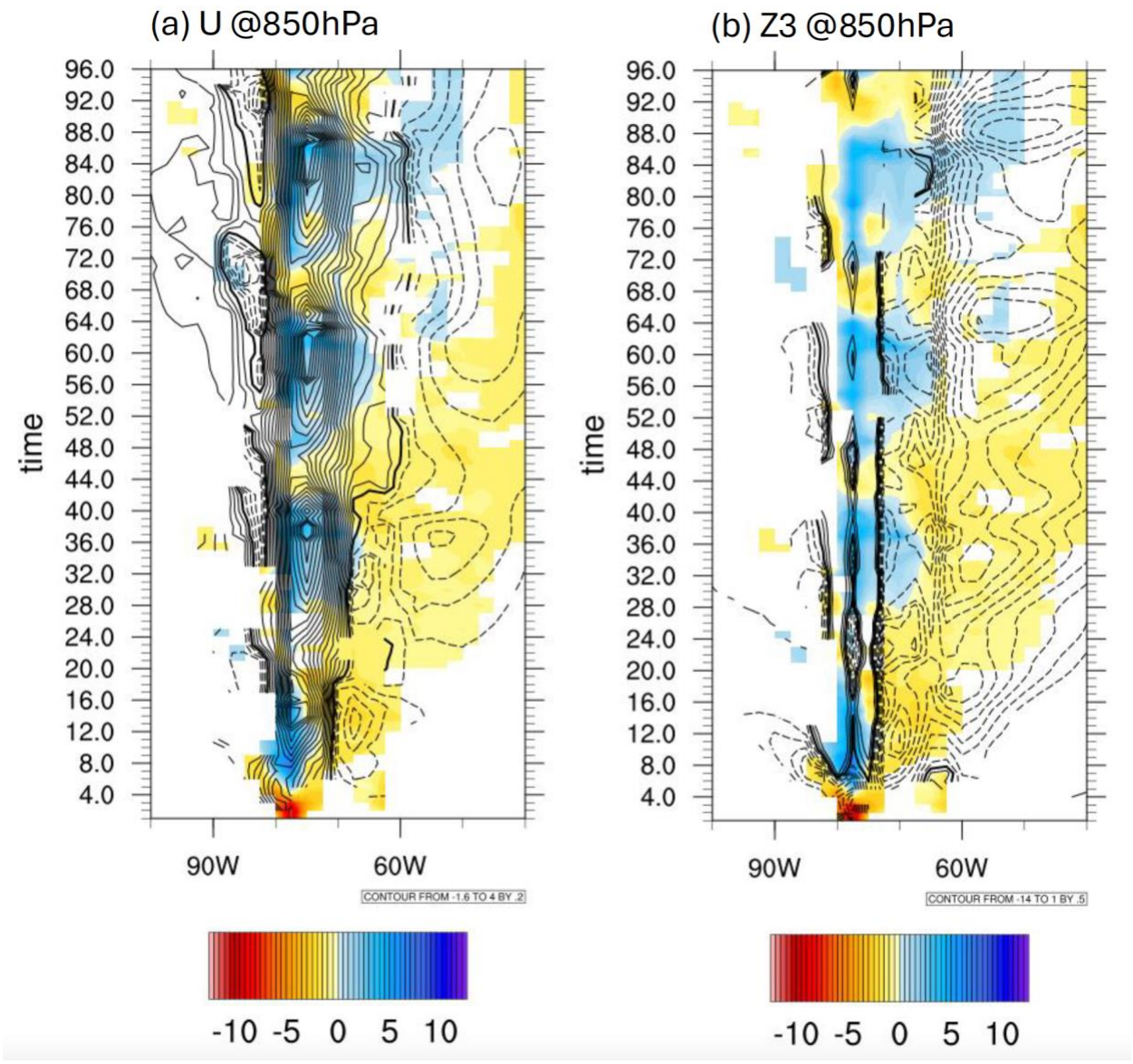

1010

An edited version of this paper was published by AGU. Published (2025) American Geophysical Union.
Qin, H., Pritchard, M., Terai, C. R., Bacmeister, J., Bogenschutz, P., & Kiladis, G. N. (2025). Remote influence of Andean convection on Amazonian rainfall and its mechanisms. Journal of Geophysical Research: Atmospheres, 130, e2025JD043465. https://doi.org/10.1029/2025JD043465

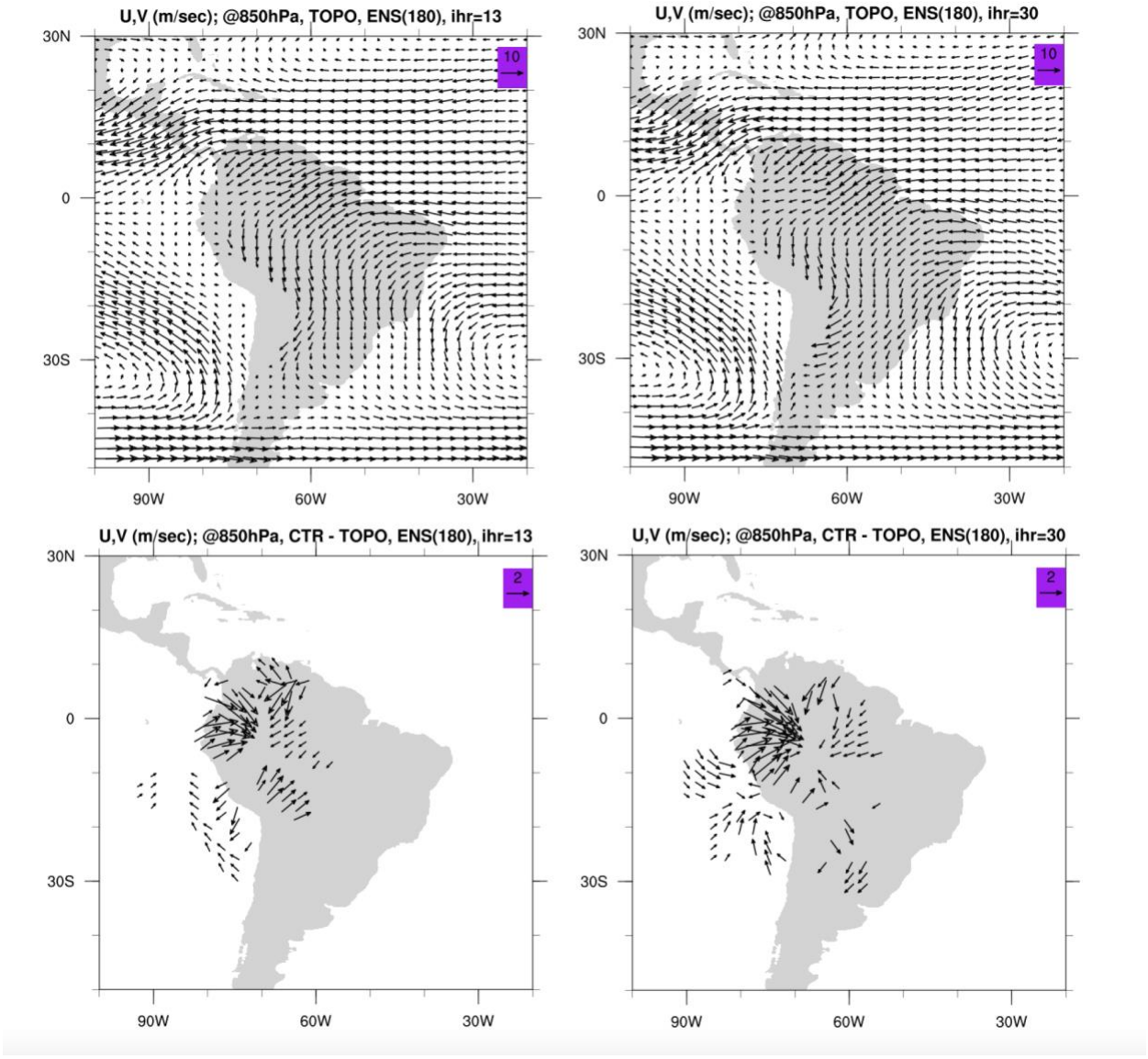

1011